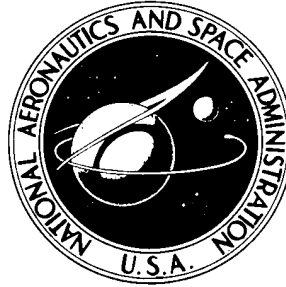


NASA TECHNICAL NOTE



NASA TN D-6036

NASA TN D-6036

FREQUENCY RESPONSES AND  
OTHER CHARACTERISTICS OF SIX  
FAST-DECAY PHOSPHORS APPLICABLE  
TO FLYING-SPOT SCANNERS

*by Charles A. Wagner*

*Flight Research Center*

*Edwards, Calif. 93523*

NATIONAL AERONAUTICS AND SPACE ADMINISTRATION • WASHINGTON, D. C. • OCTOBER 1970

1. Report No. NASA TN D-6036		2. Government Accession No.		3. Recipient's Catalog No.	
4. Title and Subtitle FREQUENCY RESPONSES AND OTHER CHARACTERISTICS OF SIX FAST-DECAY PHOSPHORS APPLICABLE TO FLYING-SPOT SCANNERS				5. Report Date October 1970	
				6. Performing Organization Code	
7. Author(s) Charles A. Wagner				8. Performing Organization Report No. H-609	
9. Performing Organization Name and Address NASA Flight Research Center P. O. Box 273 Edwards, California 93523				10. Work Unit No. 125-19-06-03-24	
				11. Contract or Grant No.	
12. Sponsoring Agency Name and Address National Aeronautics and Space Administration Washington, D. C. 20546				13. Type of Report and Period Covered Technical Note	
				14. Sponsoring Agency Code	
15. Supplementary Notes					
16. Abstract  <p>Several tests were conducted on six fast-decay phosphors to measure their characteristics applicable to flying-spot scanners. P-16, P-24, P-36, P-37, and P-SP phosphors are currently available in production cathode-ray tubes; P-X42 is an experimental phosphor. A pulse test measured rise and decay times, and two scanning tests measured frequency responses. Screen noise, burn and aging resistance, and variation of light output as a function of electron beam dwell time were also measured.</p> <p>The frequency responses of P-16, P-37, and P-SP phosphors did not vary during the tests. The frequency response of P-36 phosphor varied with electron beam dwell time, and the frequency response of P-24 phosphor varied with both dwell time and beam current. The bandwidths (frequencies at which the gain is 0.1) were as follows: P-16, 22 megahertz; P-24, 12 megahertz; P-36, 12 megahertz; P-37, 34 megahertz; P-SP, 21 megahertz.</p> <p>The bandwidth of P-X42 phosphor, too high to measure with the equipment used, was estimated to be in excess of 100 megahertz. However, this phosphor produced relatively little light and had a screen that was too noisy to be useful in flying-spot scanners.</p>					
17. Key Words (Suggested by Author(s))  Phosphors Flying-spot scanners				18. Distribution Statement  Unclassified - Unlimited	
19. Security Classif. (of this report) Unclassified		20. Security Classif. (of this page) Unclassified		21. No. of Pages 41	
				22. Price* \$3.00	

\*For sale by the Clearinghouse for Federal Scientific and Technical Information  
Springfield, Virginia 22151

# FREQUENCY RESPONSES AND OTHER CHARACTERISTICS OF SIX FAST-DECAY PHOSPHORS APPLICABLE TO FLYING-SPOT SCANNERS

Charles A. Wagner  
Flight Research Center

## INTRODUCTION

In recent years, the analysis of flying-spot scanner systems has become heavily dependent on frequency-response techniques. The effects of the cathode-ray tube (CRT) spot size, the optical system, and the film on overall system performance can be analytically described in terms of the spatial frequency responses of these elements. Reference 1 contains such an analysis. The frequency response of one important element, however, is usually unknown. This element is the phosphor screen in the cathode-ray tube.

A good deal of work, such as that discussed in reference 2, has been done in an attempt to describe the characteristics of the most common phosphors used in flying-spot scanning. Among the characteristics most often measured are decay time and efficiency. Although these characteristics are important, they give, at best, only a general idea of the frequency response of a phosphor. The frequency response is actually a complex function of rise time, decay time, and efficiency; these, in turn, may be variables depending on the energy density and the effective dwell time of the electron beam. (In scanning, dwell time is defined as spot size divided by scan speed.)

Other properties of phosphors beside the frequency response are also important for satisfactory application in a flying-spot scanner. Light output as a function of dwell time, for example, is as important for flying-spot scanners as it is for visual displays. The maximum permissible light output, aging characteristics, and screen noise are other important properties. Information of this kind is not widely available for some fast-decay phosphors, particularly the newer ones. Reference 3 describes some tests conducted on phosphors used in display cathode-ray tubes. Although the data do not apply to flying-spot scanner phosphors, some of the measured parameters and the measuring techniques are of interest.

The subject report presents the results of a series of tests conducted on six phosphors to determine their frequency responses and other properties applicable to flying-spot scanners. Four of the phosphors tested, P-16, P-24, P-36, and P-37, are registered with the Joint Electron Device Engineering Councils (JEDEC). P-X42 is an experimental phosphor that was manufactured by Westinghouse Electric Corporation, Electronic Tube Division, Elmira, N. Y. P-SP phosphor is manufactured only by Sylvania Electric Products, Inc., Electronic Tube Division, Seneca Falls, N. Y. These phosphors constitute a representative sample of those currently available with short decay times.

## THE PHOSPHOR PROBLEM

The tests of this study were designed to measure the properties of phosphors that are most important in flying-spot scanner applications. Thus it is desirable to briefly describe the characteristics of an ideal phosphor and discuss the problems introduced by actual phosphor screens. This discussion is based on the assumption that a flying-spot scanner is being used as a television camera and that the resulting video signal is being sent to a high-quality monitor.

An ideal phosphor would have zero rise and decay time; that is, it would glow with full brightness the instant it was struck with electrons and would immediately stop glowing when the electrons stopped. Actual phosphors have finite rise and decay times. Thus a spot of light on a CRT screen will accurately reproduce the size and shape of the scanning electron beam (assumed to be Gaussian) only at long dwell times (low scan speeds). At short dwell times (high scan speeds), the finite rise time limits the peak brightness of the spot to a lower value, and this peak occurs near the trailing edge of the electron beam instead of at the center. Also, the decay time causes the phosphor to continue to glow for a time after the electron beam has passed. Thus the spot of light actually grows larger and becomes distorted at the shorter dwell times. These changes affect the video signal in much the same way as a low-pass filter that has unity gain at zero frequency; that is, the frequency response of the phosphor reduces the signal amplitude and introduces a phase shift at the higher frequencies. Reduced signal amplitude appears on the monitor as a loss of contrast in areas of fine detail, and the phase shift causes the picture to smear. It is convenient to describe phosphor frequency response in terms of gain, the ratio of high-frequency signal amplitude to zero-frequency signal amplitude, and in terms of phase. It follows that an ideal phosphor would have unity gain and zero phase at all frequencies. Knowledge of gain and phase for a variety of phosphors will assist the designer of a flying-spot scanner in choosing an optimum phosphor for a given application and in constructing a video processing amplifier that will compensate, as much as possible, for these phosphor effects.

An ideal phosphor screen would also have other properties. It would produce a constant amount of light when a constant-energy electron beam was scanned over it. Actual phosphor screens have a grain structure that causes the light output to vary slightly from point to point. This variation is referred to as screen noise in this report. An ideal phosphor would strongly resist burning and aging while simultaneously producing a great deal of light over long periods at high efficiency. Actual phosphors vary in their resistance to burning and aging, maximum permissible light output, and efficiency. In applications where the dwell time varies, an ideal phosphor would have constant efficiency; that is, its light output would be independent of dwell time. Actual phosphors have efficiencies that depend on loading, which in turn is affected by dwell time. In color flying-spot scanner applications, the light from the cathode-ray tube is split into red, green, and blue color components, and these components are detected by three different photomultiplier tubes. Thus an ideal phosphor would produce white light or, at the very least, a wide emission spectrum. Actual phosphors vary considerably in their ability to meet these color requirements.

## DESCRIPTION OF APPARATUS

### Cathode-Ray Tubes

The commercially available cathode-ray tubes used in this experiment were purchased new from several manufacturers. Although they are of different types, they have similar performance characteristics. All were designed for moderately high resolution flying-spot scanning. They are all nominally 127 millimeters (5 inches) in diameter and have flat screens with minimum useful diameters of 108 millimeters (4 1/4 inches). All are electrostatically focused, magnetically deflected, and have anode voltage ratings in excess of 20,000 volts. With no deflection, best focus, and maximum beam current, all produce somewhat elliptical spots having a minor diameter less than 0.076 millimeter (0.003 inch) and a major diameter no greater than twice the minor diameter.

### Photomultiplier Tubes

Two identical photomultiplier tubes with S-20 spectral response were used. The S-20 spectral curve is shown in appendix A. Photomultiplier tube A was operated without dynode multiplication. In this mode, with its output consisting solely of the photocathode current, it served as a stable, repeatable instrument for measuring absolute light levels, but its rate of response was very low. Its sensitivity was measured and found to be 150  $\mu\text{A}/\text{lumen}$ . This sensitivity, which agrees with the manufacturer's "typical" specification, applies only when the light source is a tungsten filament bulb operated at a color temperature of 2870° K.

Photomultiplier tube B was operated with dynode multiplication for increased rate of response and greater output current. This tube was used for all relative light-output measurements and all high-speed measurements. According to the manufacturer's specifications, this photomultiplier tube has a rise time that varies from 2 nanoseconds to 4 nanoseconds over the range of dynode voltages applied during this experiment.

### Driving Circuits

The dc voltages applied to the cathode-ray tubes and the photomultiplier tubes were obtained from regulated power supplies. As an added precaution against variations in voltage, the input voltage to the power supplies was regulated with line-regulating transformers to 1 percent. With one exception, all cathode-ray tubes were tested with 22,000 volts applied to the anode.

Stable deflection and blanking amplifiers were designed especially for this experiment. They were driven from sawtooth and gate outputs of a waveform generator.

### Oscilloscope

An oscilloscope was used to measure the outputs of the photomultiplier tubes. According to the manufacturer's specifications, this oscilloscope has a nominal rise time

of 4.3 nanoseconds, measured at the input connector with the gain control set at the most sensitive position. The input impedance is 1 megohm in parallel with 15 picofarads. The vertical amplifier was sweep-tested and found to have a 3-dB bandwidth of 80 megahertz, which agrees with the manufacturer's specification. Vertical and horizontal accuracy is specified as 3 percent. Since the 4-centimeter by 10-centimeter graticule is inscribed on the inside of the CRT screen, there is no possibility of parallax error in observing traces. All traces that fall within the graticule are free from any visually detectable nonlinearities.

The anode of photomultiplier tube B was connected to the oscilloscope with a length of RG59/U (75 ohm) coaxial cable. A 75-ohm resistor was used to terminate the cable at the input to the oscilloscope. With this arrangement, a small amount of ringing at 70 megahertz was observable when very fast light pulses were input to the photomultiplier. The cable used was slightly over 1 meter long, which is about one-fourth the wavelength associated with 70 megahertz.

Considering the frequency capabilities of the individual components used in this experiment, it is estimated that the overall system bandwidth was probably in excess of 50 megahertz to -3 dB.

### Pulse Generator

For some testing, a pulse generator was used which can deliver a 50-volt pulse into a 50-ohm load with a rise time of less than 12 nanoseconds and a fall time of less than 14 nanoseconds. The pulse width was adjustable from 100 nanoseconds to 10 milliseconds, and the amplitude was continuously adjustable to zero. RG58/U (50 ohm) coaxial cable was used to connect the pulse generator to a 50-ohm load resistor. A "T" connector was inserted in the cable, and the CRT grid was connected directly to the "T" connector. In this way, very high quality pulses were obtained at the CRT grid input pin.

### Lenses

Two lenses were used. The first, used as the objective, was a four-element f/2.8 camera lens with a 50-millimeter focal length. The second was a single-element f/1.2 condensing lens with a 75-millimeter focal length.

### Targets

Two targets were used. The first was a 50-millimeter square Ronchi ruling etched on glass, with alternate black bars and clear spaces of equal width; each cycle (one bar and one space) was 0.127 millimeter (0.005 inch) wide. The second target was a slit approximately 0.25 millimeter wide.

### Dichroic Mirrors

Two red and two blue dichroic mirrors were used. The red mirrors reflected almost all light with wavelengths greater than 590 nanometers and transmitted almost

all light with shorter wavelengths. The blue mirrors reflected almost all light with wavelengths less than 500 nanometers and transmitted almost all light with longer wavelengths.

## TEST PROCEDURES

### Pulse Tests

The purpose of the pulse tests was to determine the general rise and decay characteristics of the phosphors over a wide range of electron beam energy and dwell time. The scope of these tests was limited somewhat by the available equipment. The pulse generator could not produce pulses shorter than 100 nanoseconds, although much shorter electron beam dwell times actually occur in high-speed scanning operations. As noted previously, dwell time is defined as spot size divided by scan speed. The absolute light output produced by the phosphor could not be measured because of the speed limitation of photomultiplier tube A. The rise and decay curves were observed on an oscilloscope, where the minimum-slope portions of these curves are subject to large reading errors. Even with these limitations, large differences and strong trends could be observed.

The initial pulse test on each cathode-ray tube was conducted by using a focused spot, a 20-hertz repetition rate, a pulse width of 10 microseconds, and maximum beam current. With photomultiplier tube B exposed to the light from the cathode-ray tube, the rise and decay curves were displayed on the oscilloscope. Rise time to 50 percent, 75 percent, and 100 percent of peak brightness and decay time to 50 percent and 25 percent of the brightness at the end of the pulse were recorded. The decay times were also recorded for pulse widths of 1 microsecond and 0.1 microsecond. Then the beam current was reduced until the peak light output was one-fourth its previous level, and all measurements were repeated. This sequence was continued until the light output was too low to measure. Thus rise time was measured for several driving levels ranging from the maximum capability of the cathode-ray tube down to an almost undetectable light level. Decay time was measured for all combinations of these driving levels and the three pulse widths (or dwell times).

### Scanning Tests

The scanning tests were conducted by generating a single scan line with a 60-hertz repetition rate synchronized with the power-line frequency. In this way, the effect of any 60-hertz power supply ripple was eliminated, inasmuch as all readings were taken at the same level of ripple. Each cathode-ray tube was oriented so that the direction of scan was along the minor diameter of the elliptical spot. This arrangement reduced the measured spot size and the effective electron beam dwell time to a minimum. In this report, spot size is defined as the width between the half-amplitude points of the spot profile as determined by slit-scanning.

For all scanning tests, the absolute light output of each cathode-ray tube was adjusted to a preselected standard. This standard required photomultiplier tube A to produce 0.4 microampere from the light passing through an f/5.9 clear aperture, while

the scan speed on the cathode-ray tube was about  $0.12 \text{ mm}/\mu\text{sec}$ . The actual scan speed was recorded for each tube.

For this experiment, "light output" was defined as the output current of photomultiplier tube A when the relative aperture was  $f/5.9$ . Although this definition is unusual, it appears to be more realistic than attempting a conversion to lumens. The lumen is a unit of light based on the spectral response of the human eye. Light from a flying-spot scanner cathode-ray tube is frequently detected with a photomultiplier tube having a spectral response and sensitivity fairly similar to those of an S-20 photocathode. Thus the current produced by such a photocathode from the light passing through a known aperture is considered to be a reasonable measure of effective light output.

No measurements were made of the actual electron beam energy striking the phosphor. Instead, spot size, dwell time, repetition rate, and instantaneous (not average) light output are given for each test condition. Information of this kind may be more useful to the CRT user than knowledge of electron beam energy. As a practical matter, excellent cathode-ray tubes are commercially available that can deliver enough electron beam energy to the screen to burn most phosphors under most scanning conditions and still maintain very small spot sizes. Thus the limiting factor in actual operation becomes the phosphor's capacity to absorb energy, which is directly related to its capacity to produce light.

It was not the primary purpose of this experiment to determine the maximum light output that a phosphor can safely produce. However, some maximum recommended outputs are included with the data. These recommendations are based primarily on subjective estimates of the aging rates (gradual loss of light output with constant driving conditions) observed in the phosphors over relatively short periods (less than 8 hours). The maximum recommended light output is given in terms of a load factor, which is defined in appendix B.

All scanning tests were conducted with the setup shown in figure 1. The objective lens focused the CRT spot on the target at a magnification appropriate to the test. The condensing lens formed an exit pupil (image of the objective lens) for the photomultiplier tube.

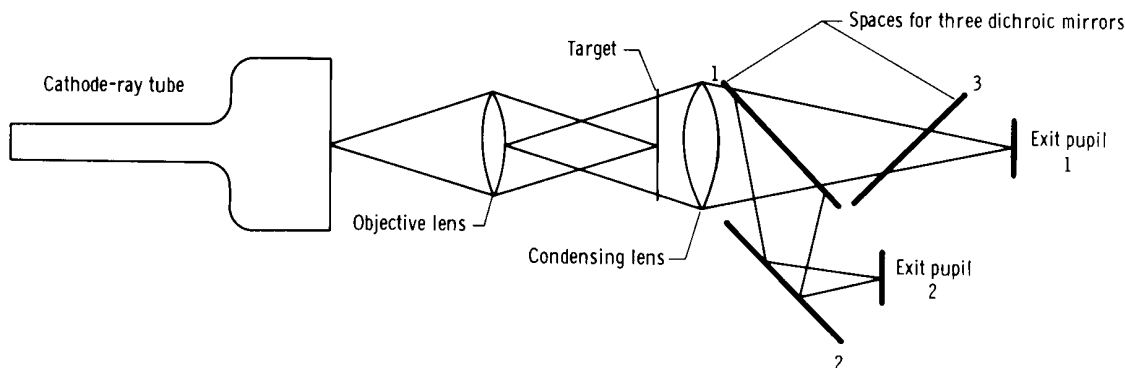


Figure 1. Scanning test apparatus.



Three of the phosphors tested, P-24, P-36, and P-SP, produced relatively wide emission spectra, which suggested that they may be suitable for applications in color flying-spot scanners. Therefore, for these phosphors, two of the scanning tests were conducted by using red, green, and blue light individually as well as unfiltered light to determine if the individual colors behaved differently from unfiltered light.

The dichroic mirrors were inserted into the spaces shown in figure 1 when individual colors were studied. Green light was obtained at exit pupil 1 when a red mirror and a blue mirror occupied spaces 1 and 3. Red light was obtained at exit pupil 2 when red mirrors occupied spaces 1 and 2. Blue light was obtained at exit pupil 2 by replacing the red mirrors with blue mirrors. The double reflection used for red and blue light was especially useful for those phosphors that had weak red or blue color components because the undesired light was discriminated against twice.

**Gain test.** — The gain test was designed to directly measure the gain of the phosphor. The test target was the Ronchi ruling, and the magnification was about 0.75. At long dwell times where phosphor effects are negligible, the CRT spot scanning the ruling produced, at the output of the photomultiplier tube, a low-frequency sine wave ac voltage riding on an average dc level. This signal was produced from the square-wave Ronchi ruling by the filtering action of the CRT spot and the modulation transfer function of the lens. Increasing the scan speed increased the output frequency, and the phosphor gain reduced the relative amplitude of the ac signal compared to the average dc level. This reduction in relative amplitude was caused solely by the phosphor gain, since only scan speed was varied during the test.

The results obtained from this test were in the form of oscilloscope waveforms similar to the waveform in figure 2. The amplitudes A and B and the frequency were recorded for a variety of scan speeds. At the lowest speed, the ratio of  $B/2A$  (which can theoretically approach unity as a maximum) was adjusted to about 0.6 by varying the magnification. This starting point assured that the low-frequency signal was adequately filtered into a pure sine wave. At higher scan speeds, the ratio of  $B/2A$  was reduced by the phosphor gain. The resulting values of  $B/2A$  were normalized to have a maximum of unity and were then plotted as a function of frequency.

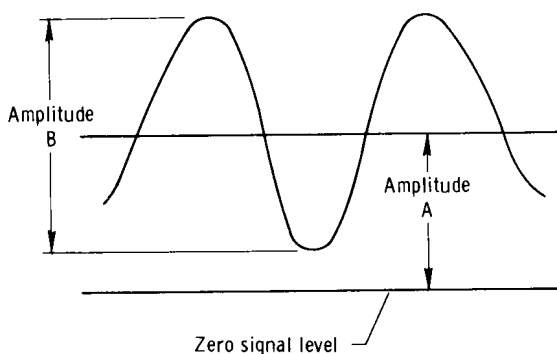


Figure 2. Typical waveform from gain test.

This test also produced information on light output. The relative values of A are a measure of relative light output as a function of dwell time. Since the absolute light output was known at one dwell time (the light output had been adjusted to a known level), the absolute light output was computed and plotted as a function of dwell time.

The gain test was conducted on the individual colors from the wide-spectrum phosphors and on the unfiltered light from all the phosphors except P-X42.

Slit-scan test. — The slit-scan test was designed to measure, indirectly, both the gain and the phase of the phosphor. The test target was the slit, and the magnification was about 15. At long dwell times (low scan speeds) where phosphor effects are negligible, the cathode-ray tube spot scanning the slit produced, at the output of the photomultiplier tube, a voltage pulse having the shape of the scanning spot. At short dwell times, this output pulse became the convolution of the low-speed spot shape with the impulse response of the phosphor. The Fourier transformation of this high-speed output pulse is the product of the frequency responses of the spot and the phosphor. The phosphor frequency response was found by dividing the frequency response obtained from the Fourier transformation by the frequency response of the spot.

The test results were in the form of photographs of oscilloscope waveforms similar to those in figure 3. A test run was made at each of three different dwell times for

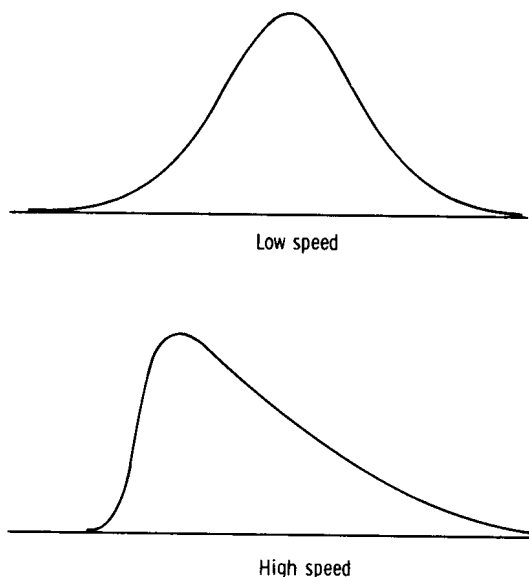


Figure 3. Typical waveforms from slit-scan test.

each test case. The low-speed photograph, which displayed practically no phosphor effects, was used to measure the spot size. The photographs obtained from the three runs and the spot size obtained from the low-speed run were used to compute the frequency response of the phosphor.

The frequency-response computations were carried out on a digital computer. For each test case, the input data to the computer consisted of the spot size, the scan speeds of the three runs, and from 20 to 30 points describing the curves on each of the three photographs. The computer was programed to compute the theoretical spot frequency response for each dwell time, assuming that the spot profile was Gaussian. The equations required for this computation are derived in appendix C. The computer also cal-

culated the Fourier transformations of the three curves, normalized to have a zero frequency gain of unity. Next, it computed the gain of the phosphor at each dwell time by dividing the gain of the appropriate Fourier transformation by the theoretical gain of the spot at a number of frequencies. The phase of the phosphor was identical to the phase of the Fourier transformation, since a Gaussian spot has zero phase at all frequencies. Finally, the computer plotted all the phosphor gain and phase curves as well as the Gaussian spot gain curves.

The slit-scan tests were conducted on the unfiltered light from each of the tested phosphors and each color component of the wide-spectrum phosphors.

Noise test. — The final test was a rough measurement of phosphor screen noise. This test, which was conducted without a target, consisted of slowly scanning the spot across the CRT screen and observing the output of the photomultiplier tube. This output was composed of a basic dc voltage with some ripple riding on it. Noise was defined as the ratio of the peak-to-peak ripple level to the average dc level stated as a percentage; it was recorded for each cathode-ray tube. It has been observed that

higher quality tubes may display much lower ripple than those used in this experiment. Presumably, a manufacturer expends more effort to obtain higher quality screens on his better quality cathode-ray tubes. However, to some extent, some phosphors may be more difficult to apply uniformly than others, and a screen noise measurement such as the one in this experiment may identify those that are exceptionally difficult to work with.

## PRECISION OF MEASUREMENTS

Aside from the inherent accuracy of the equipment used, a possible source of experimental error in these tests is the inability of an observer to locate the exact center of the oscilloscope trace. It is estimated that the maximum probable reading error is 0.1 centimeter. This error combines with the specified accuracy of the oscilloscope to give a full-scale horizontal accuracy of about 3 percent and a full-scale vertical accuracy of about 4 percent. Since all frequency measurements were made by using the full horizontal scale, they are considered to be accurate within 3 percent. Amplitude measurements in the gain tests varied from full to quarter vertical scale, and their accuracies are assumed to vary from 4 percent to 15 percent. During the slit-scan tests, it was found that the gains of Fourier transformations that were computed from different photographs of the same run never varied more than 15 percent from each other at any frequency where the data had significance. The relative light-output measurements are considered to be accurate within 10 percent of the measured values.

The data from the pulse tests were subject to greater inaccuracies than any other data. The pulses were not synchronized with the power line frequency, so there is some possibility of data scatter resulting from power supply ripple. In addition, it is difficult to accurately determine the rise time to 100 percent of peak brightness and the decay time to 25 percent of the brightness at the end of the pulse, because these curves are relatively flat in these regions. Finally, many of the decay-time measurements were made by using only a portion of the horizontal scale, so these readings may be subject to inaccuracies up to 20 percent.

## RESULTS AND DISCUSSION

### Data Format

The rise and decay times measured in the pulse tests are presented in tabular form. Unusual characteristics are pointed out in notes attached to the tables.

Figure 4 is a sample graph intended to illustrate the format of the curves presented and does not contain any actual data. The three phase curves represent those curves computed directly from the Fourier transformations of the photographs taken at the three scan speeds. These computations used the peak of the spot profile as the zero time reference. Actually, this peak may lag the center of the electron beam by a small time interval as a result of phosphor rise time. Typically, this timing error is no greater than the electron beam dwell time. Such a timing error will introduce a

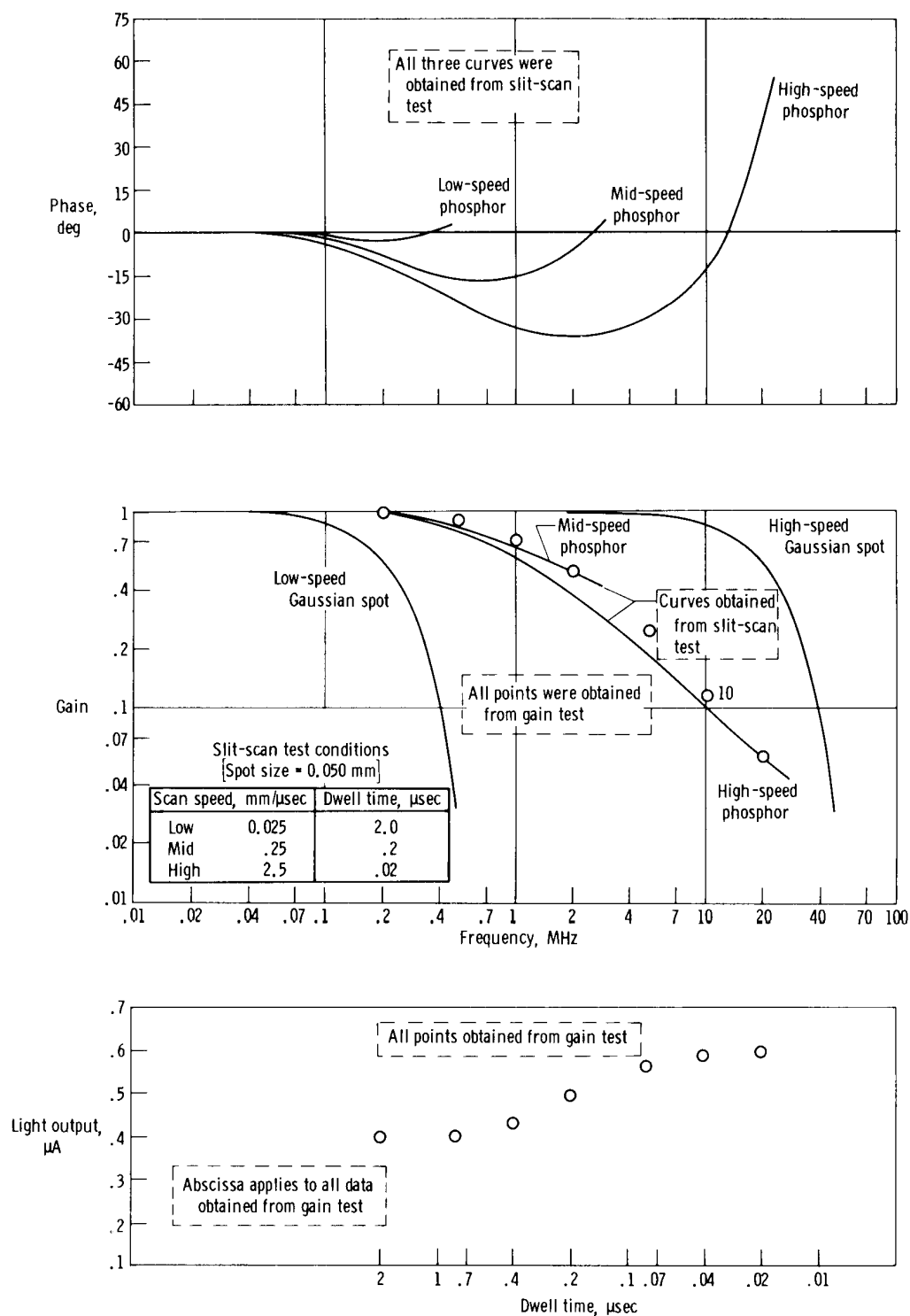


Figure 4. Sample phosphor frequency-response and light-output curves illustrating the format of the data.

high-frequency phase lead that is not actually characteristic of the phosphor. Therefore, to be theoretically correct, these curves should be modified by adding the phase lag of an appropriate time delay. No attempts were made to add this phase lag, however, inasmuch as timing errors such as these are usually insignificant in television systems.

Four gain curves are shown in figure 4. Two of the curves, labeled "Low-speed Gaussian spot" and "High-speed Gaussian spot," represent the theoretical gains of a Gaussian spot at the lowest and the highest scan speeds used in the slit-scan test. The gain of the mid-speed Gaussian spot is not shown, but its location is approximately half way between the low- and high-speed curves. The other two gain curves, labeled "Mid-speed phosphor" and "High-speed phosphor," represent the actual phosphor gains determined from the slit-scan test. The product of the "High-speed phosphor" curve and the "High-speed Gaussian spot" curve, for example, is the gain actually computed from the Fourier transformation of the high-speed slit-scan photograph. This product curve is not shown.

No low-speed phosphor gain curve is shown. The "Low-speed Gaussian spot" curve matched the Fourier transformation of the low-speed photograph closely enough that no conclusions could be drawn from the quotient of the gain curves.

The gain curve obtained from the Fourier transformation of the mid-speed photograph reached a very low value at fairly low frequencies because of the attenuation caused by the spot. Since this gain curve had no significance at higher frequencies, it was not possible to compute the "Mid-speed phosphor" gain curve at frequencies higher than those shown in the figure.

The table in the gain plot shows the conditions applicable to the three slit-scan runs. The number adjacent to the "High-speed phosphor" curve is the frequency in megahertz where the gain is 0.1. This frequency is the bandwidth of the phosphor. Although it is somewhat arbitrary to define bandwidth as that frequency at which the gain is 0.1, this definition is a practical one. In actual practice, the highest useful frequency that can be obtained from a flying-spot scanner is fairly close to the defined phosphor bandwidth.

Sample data obtained from the gain test are also shown in figure 4. The measured values of gain are shown as a series of seven discrete points that are not connected by a curve. These points may not necessarily agree with the curves obtained from the slit-scan test because the two tests were conducted under different conditions. Each point of the gain test was obtained at a different dwell time, whereas each curve of the slit-scan test was computed for one particular dwell time. In general, the lowest frequency point (the first) of the gain test was obtained under approximately the same conditions as were used in the low-speed slit-scan test. Similarly, the conditions for the fourth and seventh points were approximately the same as the conditions for the mid-speed and high-speed slit-scan tests, respectively. Thus it is expected that the fourth and seventh discrete points should fall, respectively, on the "Mid-speed phosphor" and "High-speed phosphor" curves.

The bottom plot of figure 4 shows the values of light output obtained from the gain test. These values are plotted on a dwell-time abscissa. It can be seen that the seven light-output points are vertically aligned with the seven gain points. This arrangement

was chosen because each light-output point was obtained from the same test run as the gain point directly above it. Thus the dwell times used in the gain test can be read on the abscissa of the light-output plot.

Other data such as screen noise, maximum recommended light output, and color are included in the discussion of each phosphor. The maximum recommended light output is given in terms of a load factor, which is defined in appendix B. The color was determined by subjective visual observation; spectral curves are presented in appendix A.

Some phosphors displayed characteristics that required variations in data format and content for an adequate description. These exceptions are explained for each phosphor.

### P-16 Phosphor

Table 1 shows the results of the pulse test on P-16 phosphor. Allowing for some scatter in the data from experimental errors, it is seen that the rise time and decay time do not depend significantly on electron beam energy, but the decay time does seem to decrease somewhat as the pulses get shorter.

TABLE 1. - PULSE DATA FOR P-16 PHOSPHOR

Relative light output	Rise time, $\mu\text{sec.}$ to -			Decay time, $\mu\text{sec.}$ to -		Pulse width, $\mu\text{sec.}$
	50 percent	75 percent	100 percent	50 percent	25 percent	
1	0.040	0.100	1.0	0.040 .038 .032	0.150 .135 .060	10 1 .1
1/4	0.035	0.085	0.8	0.040 .036 .032	0.150 .105 .060	10 1 .1
1/16	0.035	0.080	0.8	0.040 .035 .035	0.150 .100 .060	10 1 .1
1/64	0.040	0.110	1.0	0.040 .035 .035	0.160 .100 .060	10 1 .1

Figure 5 shows the frequency response obtained for P-16 phosphor, as well as the variation in light output. All the gain data agree within the accuracy of this experiment. These data show that the gain is reasonably independent of dwell time. They also show that the bandwidth of P-16 phosphor is about 22 megahertz. The light output increases about 40 percent as the dwell time is decreased by a factor of 100.

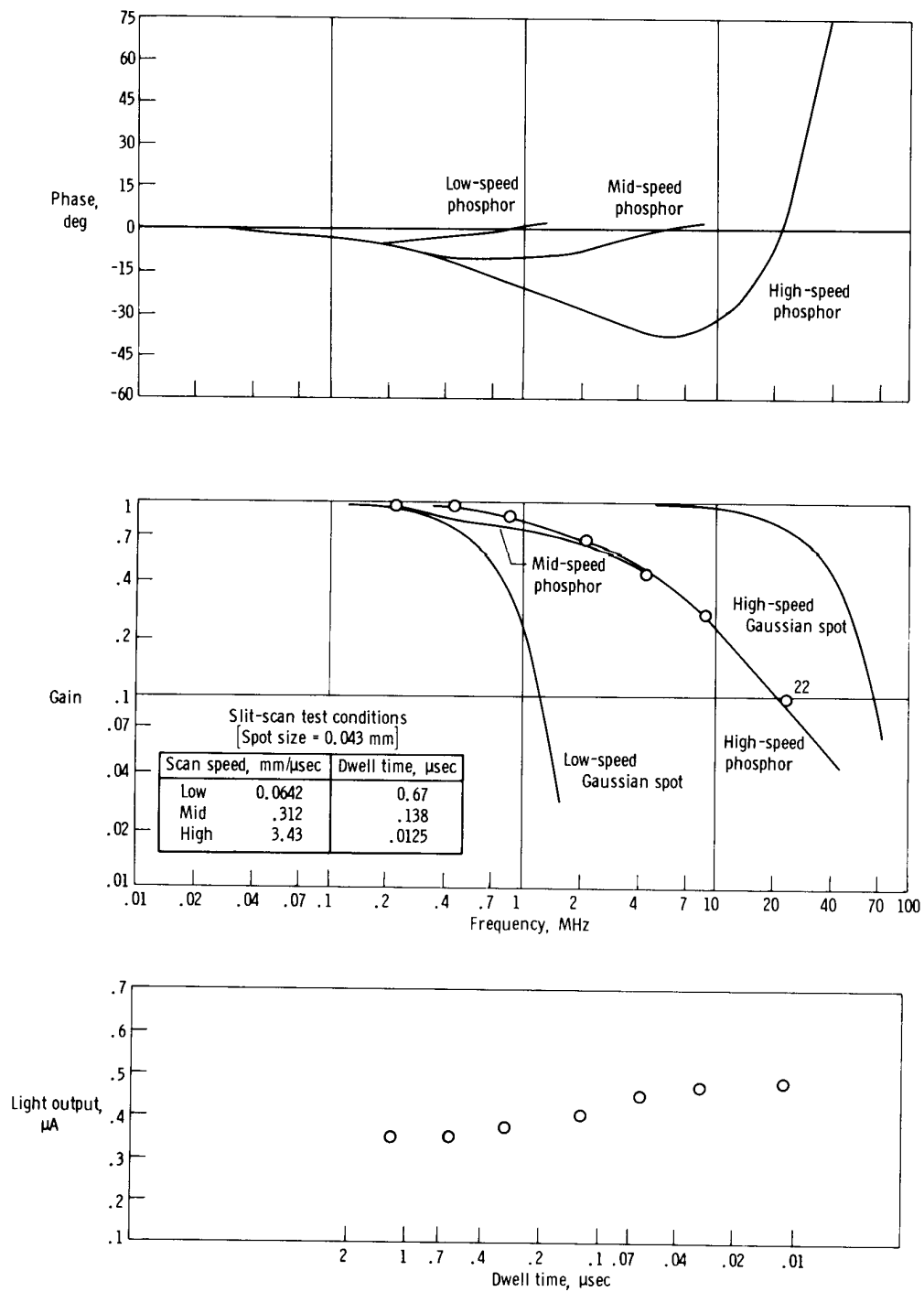


Figure 5. P-16 phosphor frequency response and light output.

The following characteristics were measured:

Spot size in direction of scan . . . . .	0.043 mm
Spot size normal to scan . . . . .	0.043 mm
Noise level . . . . .	20 percent
Color of emitted light . . . . .	Bluish purple

P-16 phosphor ages very rapidly. The shorter dwell times caused about a 15-percent loss in light output after about 2 hours of operation, and the longer dwell times caused a 50 percent loss in one-half hour. The maximum recommended load factor is  $0.0015 \mu\text{A}/\text{mm}^2$  at a dwell time of 0.5 microsecond. Even at this loading, aging occurs at a moderately high rate. However, it appears that the rate of aging reduces with time, and that the light output more or less stabilizes after several days of operation.

This phosphor burns relatively easily. At a dwell time of about 2.2 microseconds, the phosphor burned rapidly. It also burned during some of the higher energy pulse tests at higher repetition rates.

#### P-24 Phosphor

The results of the pulse test on P-24 phosphor are shown in table 2. Allowing for some scatter in the data from experimental errors, several conclusions can be drawn.

TABLE 2. - PULSE DATA FOR P-24 PHOSPHOR

Relative light output	Rise time, $\mu\text{sec.}$ to -			Decay time, $\mu\text{sec.}$ to -		Pulse width, $\mu\text{sec.}$
	50 percent	75 percent	100 percent	50 percent	25 percent	
1	0.10	0.25	2.0	0.10 .10 .08	0.35 .30 .21	10 1 .1
1/4	0.15	0.40	3.0	0.20 .18 .13	0.55 .46 .34	10 1 .1
1/16	0.12	0.40	3.5	0.30 .25 .15	0.80 .65 .40	10 1 .1
1/64	0.10	0.12	0.2	0.40 .30 .14	1.0 .8 .4	10 1 .1

The first is that the rise time varies considerably with electron beam energy, reaching a maximum at moderate loading and decreasing for both heavy and light loading. In addition, the shape of the rise curve also varies with loading. For example, the phosphor requires about 30 times as much time to reach 100 percent as it does to reach 50 percent of peak brightness for the 1/16 light output, but it requires only twice as much time to reach 100 percent as it does to reach 50 percent of peak brightness for the 1/64 light output.



Other conclusions can be reached by observing the decay times. The shape of the decay curve appears to be fairly constant over the range of the data. Decay to 25 percent requires between 2 1/2 and 3 times as much time as decay to 50 percent of the brightness at the end of the pulse in almost all instances. However, the decay time itself increases with increasing pulse width and decreasing load. A closer study discloses that, at higher loads, decay time is heavily dependent on loading and only slightly dependent on pulse width. Conversely, at lower loads, decay time is heavily dependent on pulse width and only slightly dependent on loading.

Figure 6 shows the frequency response obtained for P-24 phosphor, as well as the light-output variation. The gains vary considerably with each other. The "Mid-speed phosphor" curve, for example, is higher than the "High-speed phosphor" curve. The discrete points from the gain test suggest a still higher curve. The fourth point is higher than the "Mid-speed phosphor" curve, and the seventh point is higher than the "High-speed phosphor" curve. Thus the results of the gain test and the results of the slit-scan test do not agree.

One fact tends to explain the apparent disagreement between the fourth and seventh points and their respective phosphor curves. At the lowest scan speed in the gain test, the CRT spot actually grew larger than it was at the next higher speed. This spot growth probably occurred because, at long dwell times, phosphor that was not actually struck by electrons was excited by nearby glowing phosphor and also began to glow. The net effect was that the gains measured by the gain test at the lowest frequencies were slightly lower than they would have been if this spot growth had not occurred. In the absence of this growth, the maximum gain would be larger, and normalizing the gains would cause the higher frequency points to be lower. Thus, the fourth point would agree more closely with the mid-speed curve and the seventh point would agree more closely with the high-speed curve.

The decay times, as measured by the pulse test, suggest that long dwell times should decrease the bandwidth, since the decay time increases with increasing dwell time. However, the curves of figure 6 contradict this suggestion, since the higher bandwidths appear to be associated with long dwell times. This contradiction can be explained in terms of that portion of the decay curve that follows the 25-percent decay point. Although no precise measurements were made, P-24 phosphor did seem to have an exceptionally long decay tail of relatively low amplitude. This tail contained only a relatively small fraction of the total spot energy at long dwell times. But at short dwell times, the fraction of energy in the long decay tail became large enough to adversely affect the phosphor's bandwidth.

At first glance, it appears that the highest bandwidth could be obtained from P-24 phosphor by using a low scan speed to obtain long dwell times. Although this is true, it is not practical because the gain obtained from scanning is actually the product of the phosphor and spot gains. At long dwell times, the spot gain is low and limits the overall bandwidth.

Another method of improving the bandwidth of P-24 phosphor is suggested by the pulse data. Apparently, decay time can be reduced by increasing the electron beam energy. Since the cathode-ray tube tested could not produce more beam energy than was required for the slit-scan test, a second tube was used for further testing. This tube was of the same general class as the first, but it was a much more expensive,

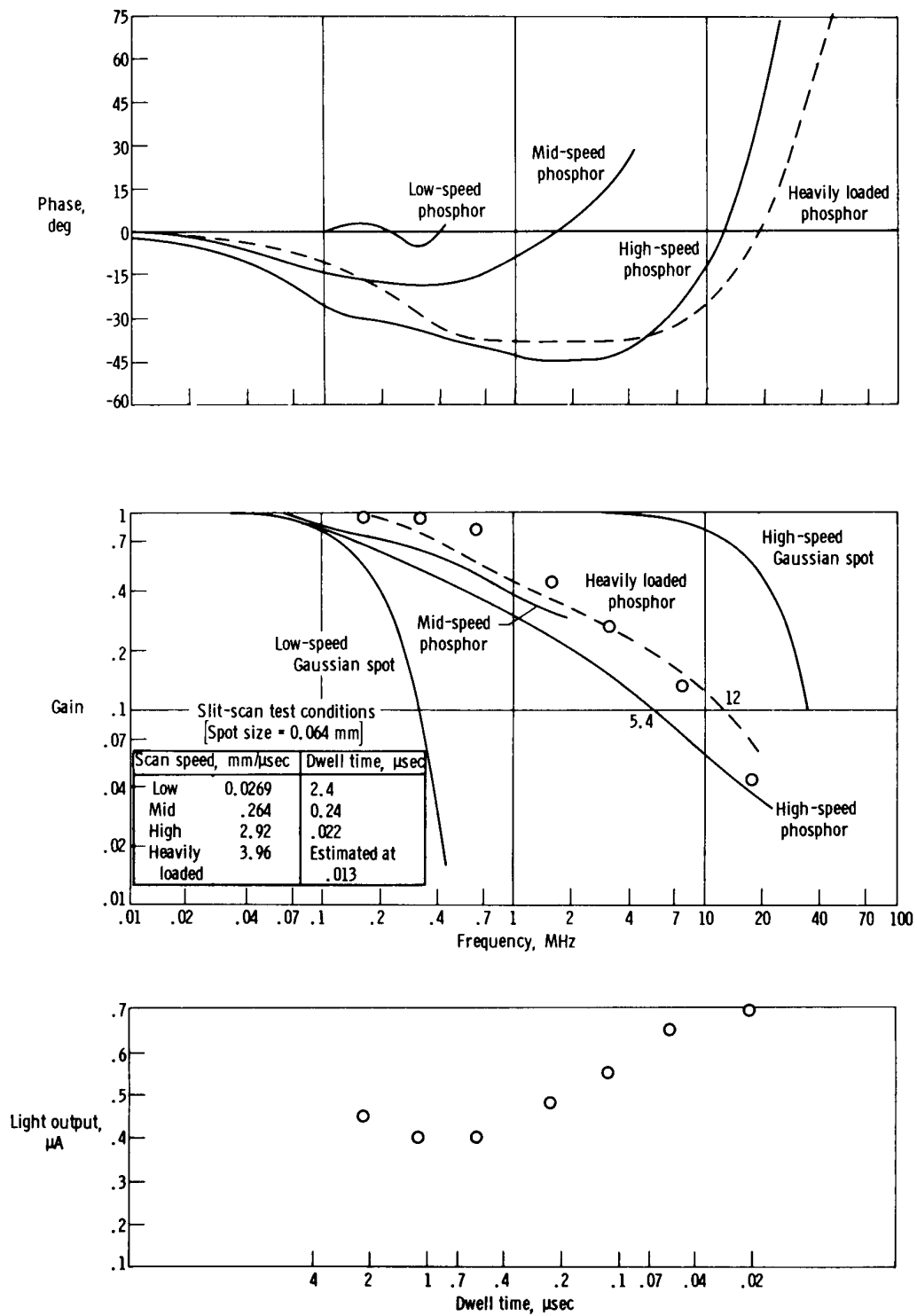


Figure 6. P-24 phosphor frequency response and light output.

higher quality unit capable of delivering more beam energy to the screen in a smaller diameter spot. This cathode-ray tube was borrowed from another project and could not be mistreated. To avoid the risk of burning the phosphor, no tests were conducted with high beam current and low scan speeds, but a high-speed slit-scan test was conducted at maximum beam current. The computed frequency response of the phosphor, corrected for the approximate effects of the spot size (estimated at 0.05 mm), is shown in figure 6 as a pair of dashed curves labeled "Heavily loaded phosphor." The bandwidth is 12 megahertz, compared to the previous value of 5.4 megahertz. The light-output load factor was about 7 times greater than that of the previous test. A second test was conducted on this cathode-ray tube at a load factor equal to that of the first tube. The resulting bandwidth reduced to that produced by the first tube, indicating that the phosphors in the two cathode-ray tubes were identical in bandwidth characteristics, at least at one load factor. Other tests showed that bandwidths lower than 5.4 megahertz are obtained at lower load factors. It is possible that bandwidths higher than 12 megahertz may be obtainable at very high load factors, but such tests were beyond the capabilities of the equipment available for this experiment.

The light output increases up to 75 percent with decreasing dwell time. The slight increase in light output at the longest dwell time was probably caused by the spot growth discussed previously.

The gain test and the slit-scan test were also conducted on each of the individual colors of the light from P-24 phosphor. All results were identical to the results obtained with unfiltered light. The relative signal levels in the photomultiplier tube from the three colors were as follows:

Red . . . . .	7 percent
Green . . . . .	50 percent
Blue . . . . .	43 percent

The following characteristics were measured for the first cathode-ray tube:

Spot size in direction of scan . . . . .	0.064 mm
Spot size normal to scan . . . . .	0.128 mm
Noise level . . . . .	8 percent
Color of emitted light . . . . .	Green

This phosphor did not age noticeably during any of the tests. It was also very resistant to burning. None of the tests resulted in screen damage, even though very long dwell times were tried and high repetition rates were applied to the most severe pulse tests. The maximum recommended load factor is  $0.003 \mu\text{A}/\text{mm}^2$  at a dwell time of 0.5 microsecond. This load factor was chosen because spot growth occurred at higher loads.

The characteristics of P-24 phosphor are such that it can be operated safely at high load factors where maximum bandwidth is obtained. Under these conditions, it will produce a great deal of light, which usually contributes to a good signal-to-noise ratio at the output of the photomultiplier tube.

## P-36 Phosphor

Table 3 shows the results of the pulse test on P-36 phosphor. Allowing for some scatter in the data resulting from experimental errors, several conclusions can be drawn. The first is that the rise time decreases with increasing beam energy. For long pulses, the decay time increases with decreasing beam energy. For short pulses, the decay time is fairly constant for varying beam energy. Increasing pulse width always increases decay time, but this effect is more pronounced at the lower beam energies. The rise and decay times, however, are not sufficient to describe the time-dependent characteristics of this phosphor because of the loss of light output under constant loading described in the footnote of table 3. This characteristic looks like a type of decay, which makes it difficult to relate rise and decay times to the frequency response.

TABLE 3. - PULSE DATA FOR P-36 PHOSPHOR

Relative peak light output (a)	Relative light output after 10 $\mu$ sec, percent (a)	Rise time, $\mu$ sec, to -			Decay time, $\mu$ sec, to -		Pulse width, $\mu$ sec
		50 percent	75 percent	100 percent	50 percent	25 percent	
1	30	0.10	0.20	0.80	0.12 .06 .04	0.50 .24 .10	10 1 .1
1/4	63	0.20	0.44	2.0	0.18 .07 .05	0.65 .30 .14	10 1 .1
1/16	95	0.80	1.6	4.0	0.20 .14 .05	0.80 .50 .10	10 1 .1

<sup>a</sup>P-36 phosphor responded to pulses by rising to a peak light level, and then, with the pulse still on, the light level began to decrease. The relative peak light output compares the peak values of light reached during the various pulses. The relative light output after 10  $\mu$ sec is the pulse amplitude after 10  $\mu$ sec compared to its own peak, which occurred earlier during that same pulse.

Figure 7 shows the frequency response obtained for P-36 phosphor, as well as the light-output variation. The gains vary considerably with each other. The "Mid-speed phosphor" curve is higher than the "High-speed phosphor" curve, showing that P-36 phosphor, like P-24 phosphor, has increased bandwidth at longer dwell times. The fourth discrete point of the gain test closely matches the "Mid-speed phosphor" curve, and the seventh point closely matches the "High-speed phosphor" curve. Thus the results of the gain and slit-scan tests agree. The bandwidth of P-36 phosphor is 12 megahertz for dwell times between 0.01 microsecond and 0.04 microsecond. Extrapolating from the known data, it is logical to assume that the bandwidth probably decreases slightly for shorter dwell times and increases slightly for longer dwell times. However, since the scanning gain is the product of the spot and phosphor gains, and since the spot gain causes low bandwidth at long dwell times, the scanning bandwidth has a maximum near 12 megahertz.

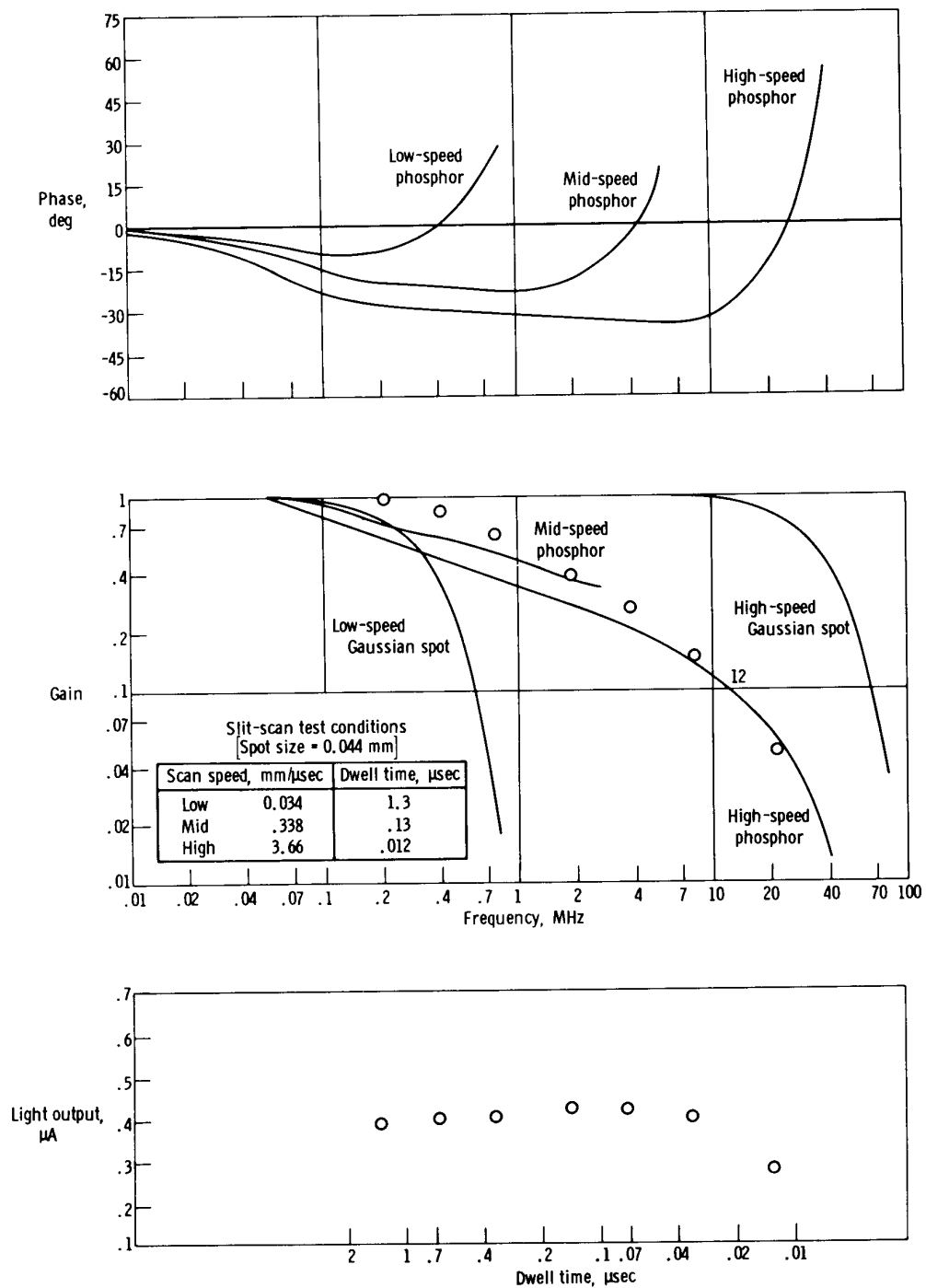


Figure 7. P-36 phosphor frequency response and light output.

The light-output curve has a relative maximum around a dwell time of 0.1 microsecond. Longer dwell times result in a slight loss of light output, and shorter dwell times cause a sharp loss of light output. At a dwell time of 0.013 microsecond, the light output is only 67 percent of the maximum. This trend is still more pronounced at shorter dwell times.

The gain test and the slit-scan test were also conducted on each of the individual colors of the light from P-36 phosphor. These tests showed that each color behaved much differently from unfiltered light. In fact, the three colors could be considered three different phosphors. Figures 8 to 10 show the frequency responses of the individual colors. All the scanning conditions for each color test duplicated the corresponding conditions for the test using unfiltered light. However, the measured spot size changed from color to color. The measured values were as follows:

Unfiltered light . . . . .	0.044 mm
Red light . . . . .	0.049 mm
Green light . . . . .	0.044 mm
Blue light . . . . .	0.041 mm

Since this variation did not occur during the color tests of the other phosphors, poor color correction in the optical system was probably not the cause. Instead, the non-linear, color-sensitive properties of this phosphor probably resulted in a larger area emitting red light than the area emitting blue light.

The gain curves in figures 8 to 10 show that the bandwidth varies from 3.8 megahertz for red light to 18 megahertz for green light to 26 megahertz for blue light. The red light is the only color that has a large increase in bandwidth with increased dwell time. The variations for green and blue light are not considered significant, inasmuch as they agree within the experimental accuracy. The seventh point that should have been obtained from the gain test on the red light was too small to be readable on the oscilloscope. However, the fourth point should agree with the "Mid-speed phosphor" curve. The point is actually slightly high, probably because of spot growth similar to that described for P-24 phosphor.

Figure 11 shows all the light-output curves for the three colors. Two strong trends are evident. First, the light exhibits a spectral shift toward the red as dwell time is decreased. Second, at short dwell times, the light output of each color decreases rapidly.

The following characteristics were also measured:

Spot size normal to scan for all the light . . . . .	0.088 mm
Noise level . . . . .	7 percent
Color of emitted light . . . . .	Yellow

P-36 phosphor lost about 10 percent of its light output during the tests. In addition, it burned slowly when a dwell time of 3.4  $\mu$ sec was used. Similarly, the highest energy pulse test also caused either slow burning or rapid aging. The maximum recommended load factor is 0.003  $\mu$ A/mm<sup>2</sup> at a dwell time of 0.5 microsecond. Thus, P-36 phosphor has moderately high resistance to burning and aging.

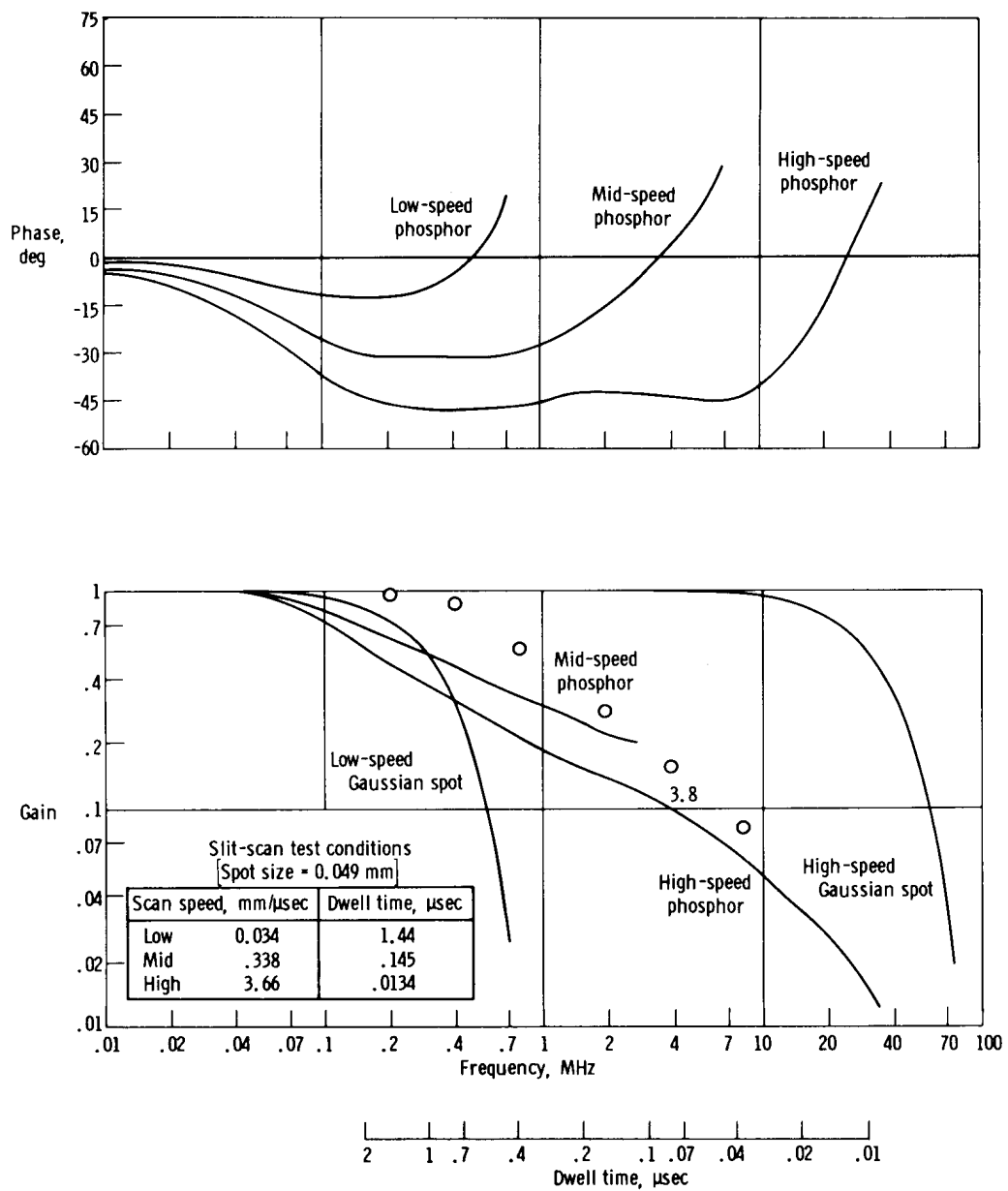


Figure 8. P-36 phosphor red-light frequency response.

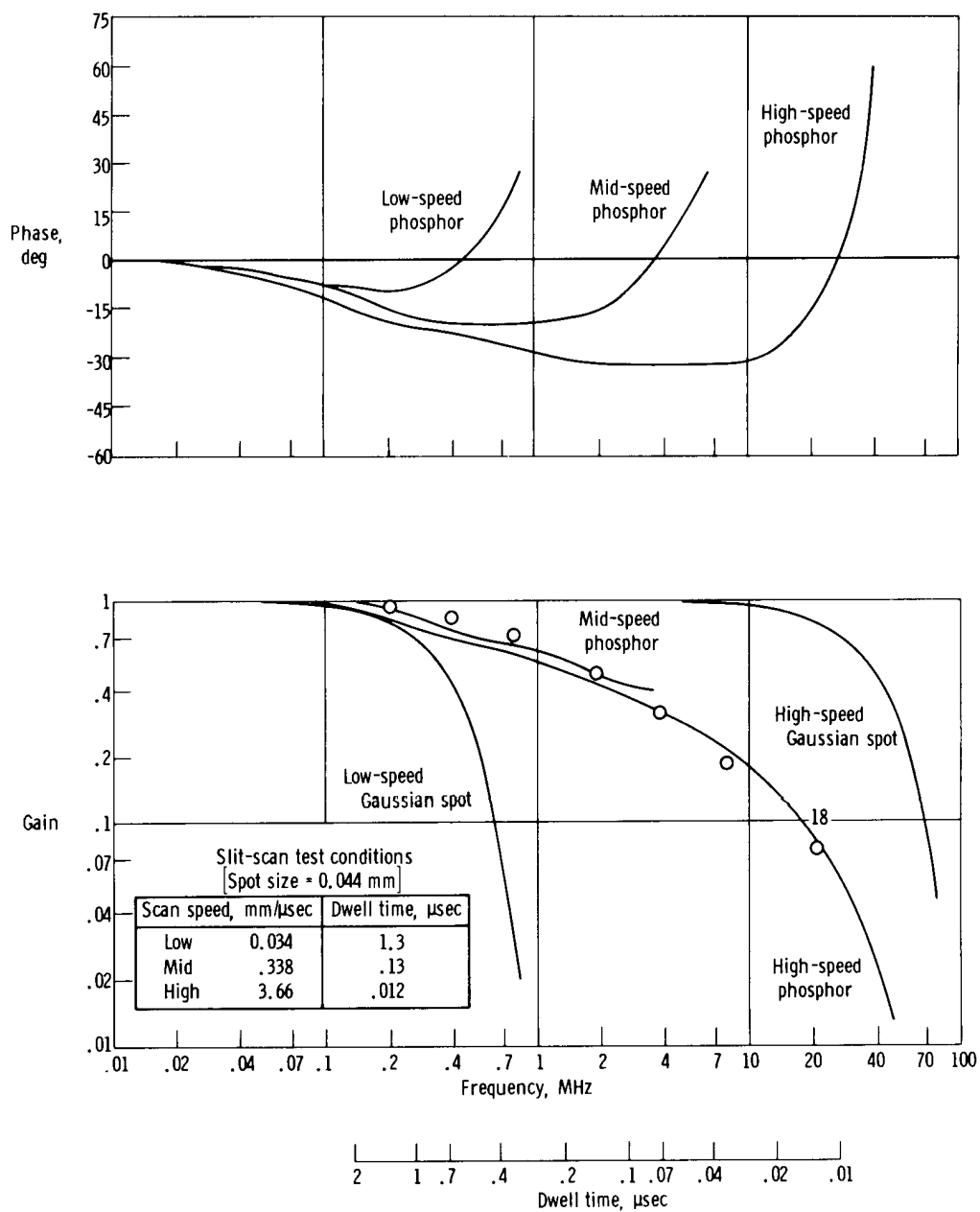


Figure 9. P-36 phosphor green-light frequency response.



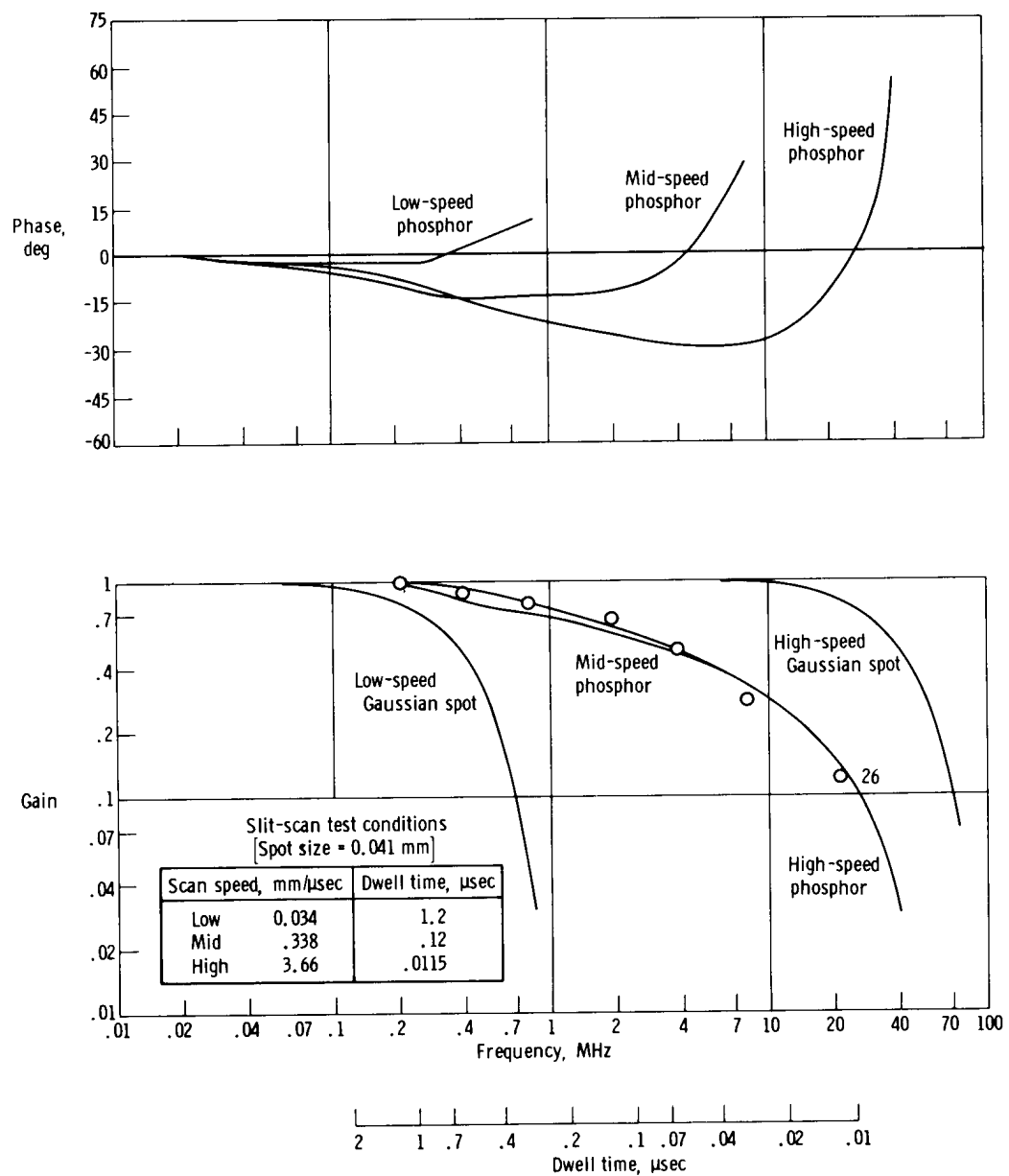


Figure 10. P-36 phosphor blue-light frequency response.

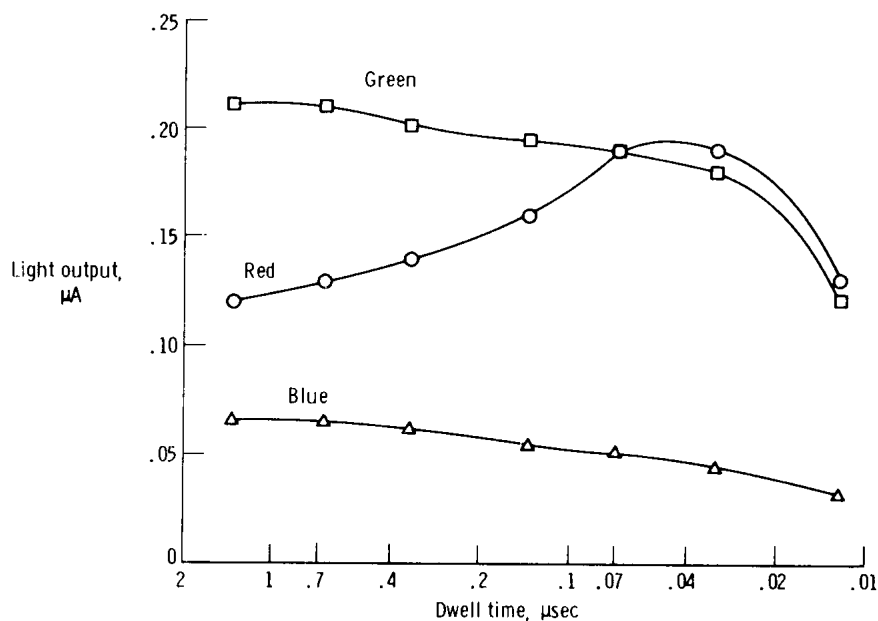


Figure 11. P-36 phosphor color light output.

### P-37 Phosphor

Table 4 shows the results of the pulse test on P-37 phosphor. Allowing for some scatter in the data from experimental errors, several conclusions can be drawn. The first is that the rise time decreases with increasing beam energy. Long pulses result in longer decay times than short pulses. Beam energy has only a small effect on decay time, and this effect occurs only at very low beam energy. The rise and decay times,

TABLE 4. - PULSE DATA FOR P-37 PHOSPHOR

Relative peak light output (a)	Relative light output after 10 μsec, percent (a)	Rise time, μsec, to -			Decay time, μsec, to -		Pulse width, μsec
		50 percent	75 percent	100 percent	50 percent	25 percent	
1	18	0.05	0.12	0.60	0.08 .04 .03	0.25 .14 .07	10 1 .1
1/4	63	0.15	0.40	2.0	0.08 .06 .035	0.25 .20 .08	10 1 .1
1/16	98	0.60	1.2	4.0	0.10 .08 .03	0.32 .26 .06	10 1 .1

<sup>a</sup>P-37 phosphor responded to pulses by rising to a peak light level, and then, with the pulse still on, the light level began to decrease. The relative peak light output compares the peak values of light reached during the various pulses. The relative light output after 10 μsec is the pulse amplitude after 10 μsec compared to its own peak, which occurred earlier during that same pulse.

however, are not sufficient to describe the time-dependent characteristics of this phosphor because of the loss of light output under constant loading described in the footnote of table 4. This characteristic looks like a type of decay, which makes it difficult to relate rise and decay times to the frequency response.

Figure 12 shows the frequency response and the light-output variation obtained for P-37 phosphor. All the gain curves agree within the accuracy of this experiment. These curves show that the gain is reasonably independent of dwell time. They also show that the bandwidth of P-37 phosphor is about 34 megahertz. The light output decreases about 60 percent as the dwell time is decreased by a factor of 100.

The following characteristics were measured:

Spot size in direction of scan . . . . .	0.040 mm
Spot size normal to scan . . . . .	0.060 mm
Noise level . . . . .	18 percent
Color of emitted light . . . . .	Blue

This phosphor did not age or burn during the tests, although a load was applied that was three times the maximum load of the gain test. From this it was difficult to determine a maximum recommended load; however, an experienced observer can frequently determine a reasonable loading level for a phosphor by observing the raster. This method is, of course, highly subjective. The maximum recommended loading determined by visual observation is about  $0.005 \mu\text{A}/\text{mm}^2$  at a dwell time of 0.5 microsecond.

#### P-X42 Phosphor

P-X42 phosphor was the most unusual phosphor tested. The test procedures used on the other phosphors were unsuitable for P-X42 phosphor because of several of its characteristics. First, it had the fastest rise and decay times and the highest bandwidth of all the phosphors tested. In fact, the bandwidth of the test equipment was inadequate to measure the speed of this phosphor. Second, P-X42 phosphor had such high screen noise that the gain test could not be used. The screen noise was about 100 percent; that is, the light output varied from 50 percent to 150 percent of the "average" level during scanning. Third, P-X42 phosphor exhibited a relatively low efficiency. This characteristic made it impossible to obtain the same light output as was obtained from the other phosphors. Fourth, the low-speed spot profile was very different from Gaussian. All the other phosphors produced low-speed spot profiles that were reasonably close to Gaussian.

Table 5 shows the results of the pulse test on this phosphor. The only conclusions that can be reached with confidence are that the decay time increases with increasing pulse width, and the shape of the rise curve varies with beam energy. The rise and decay times shown in the table may be somewhat too long, since the rise time of the measuring circuit probably affected the results.

For the slit-scan test, the light output, which was adjusted to the maximum capability of the cathode-ray tube, was 0.035 microampere. This low light output, which is less than 10 percent of the outputs of the other phosphors, was caused by two factors.

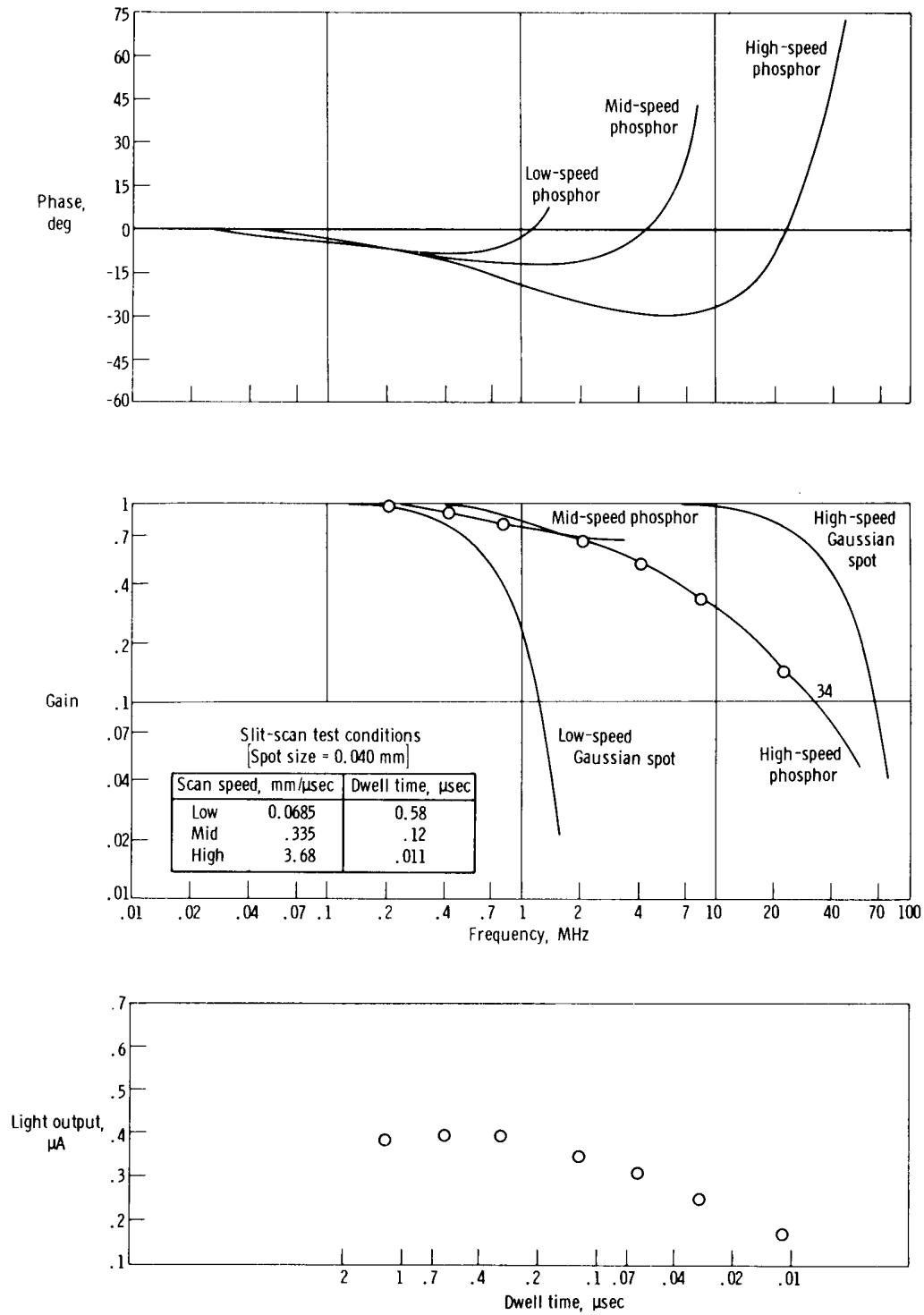


Figure 12. P-37 phosphor frequency response and light output.

TABLE 5. -- PULSE DATA FOR P-X42 PHOSPHOR

Relative light output	Rise time, $\mu\text{sec.}$ to -			Decay time, $\mu\text{sec.}$ to -		Pulse width, $\mu\text{sec.}$
	50 percent	75 percent	100 percent	50 percent	25 percent	
1	0.02	0.16	2.0	0.020 .020 .014	0.040 .040 .022	10 1 .1
1/4	0.02	0.25	2.0	0.020 .016 .010	0.040 .040 .020	10 1 .1
1/16	0.02	0.35	2.0	0.020 .016 .012	0.040 .040 .020	10 1 .1

First, as mentioned previously, the efficiency of the phosphor is low. Second, the anode of the cathode-ray tube was operated at only 15,000 volts, compared to 22,000 volts for the other tubes. This low-voltage operation was necessary because the spot could not be focused at higher anode voltages without exceeding the rated voltage of the focus electrode. The light output was found to be constant, completely independent of dwell time, repetition rate, or any other variable except beam energy. Thus it was unnecessary to plot light output.

The results of the slit-scan test on P-X42 phosphor were not similar to the results obtained from the other phosphors. At all except the very shortest dwell times, the spot size and shape did not change enough to measure. This result strongly suggests that P-X42 phosphor has a gain of unity over a wide frequency range. Figure 13 shows the only meaningful results obtained from the slit-scan test. Curves A and B are the actual Fourier transformations of the spot profiles obtained at relatively long and short dwell times, respectively. Curve C, which is curve A shifted to the right by an amount equal to the ratio of the two dwell times, is the theoretical prediction of curve B if no frequency attenuation had occurred. Gain curve D, which is curve B divided by curve C, shows the attenuation that actually occurred between the two test cases. It is observed that curve D is down only 3 decibels at 40 megahertz. This curve is the gain of P-X42 phosphor, the photomultiplier tube, the oscilloscope, and the interconnecting circuit, all in series. Each element probably contributes significantly to this result, and it is not possible to determine the relative contribution of each. But it is certain that the bandwidth of P-X42 phosphor is at least 80 megahertz, and an extrapolation suggests that it may be well in excess of 100 megahertz. Also, this result shows that the test circuit is adequate to at least 40 megahertz.

The phase curves also follow these results. The shape of curve A, when shifted to the curve C position, is similar to that of curve B. Such close agreement suggests that the variations in curve A are caused by such time-independent factors as the optical system and the actual profile of the electron beam. These variations are closely preserved at the shorter dwell time. For clarity, the phase angle curve D was not shown in figure 12. However, since curve D would be the difference between curves B and C, it can be seen that the phase of the phosphor and the measuring circuit in series is within  $\pm 2^\circ$  up to 40 megahertz.

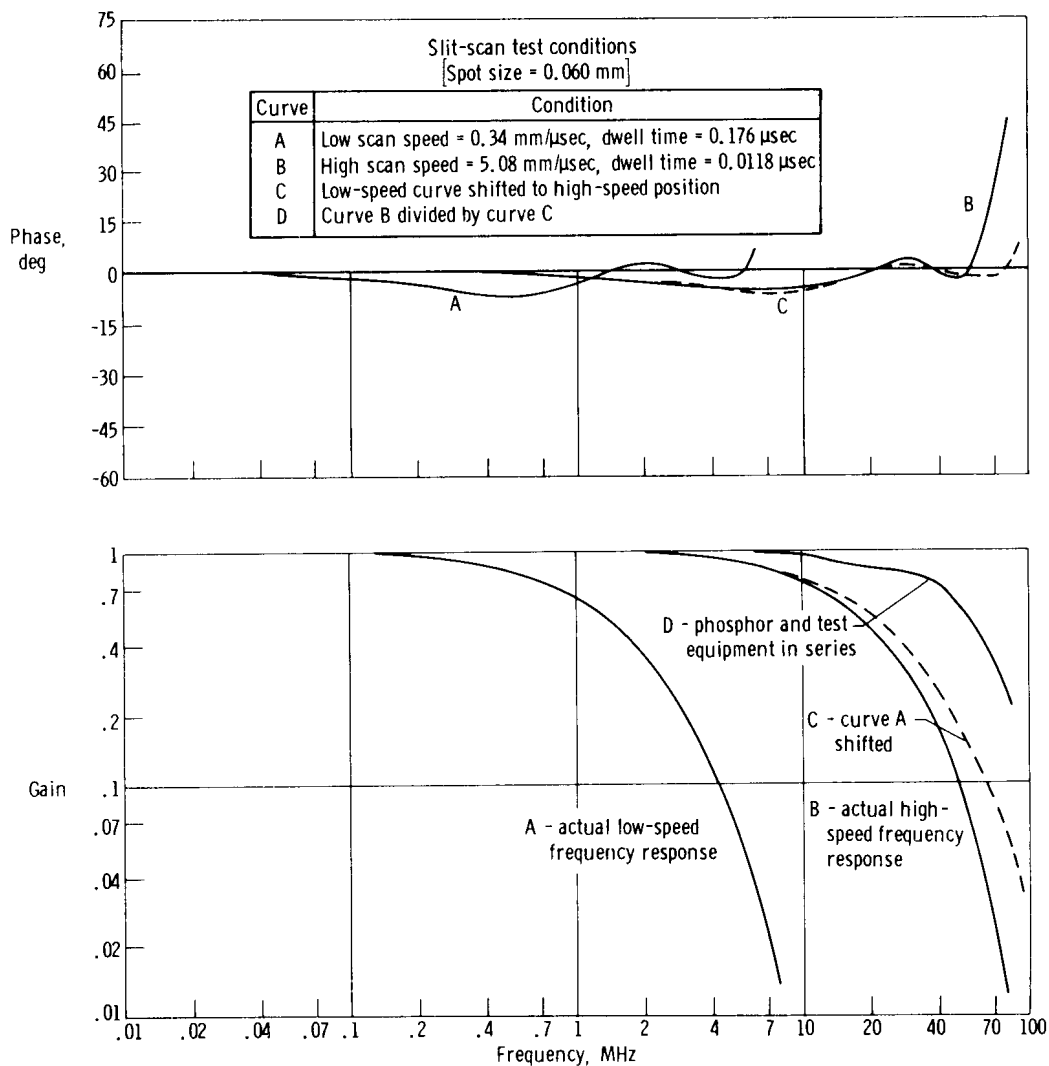


Figure 13. P-X42 phosphor frequency response.

The following characteristics were measured:

Spot size in direction of scan . . . . . 0.060 mm  
 Spot size normal to scan . . . . . 0.060 mm  
 Color of emitted light . . . . . Green

No spectral distribution curves were available from the manufacturer of this phosphor; however, the color appeared to be similar to that of P-24 phosphor. A slightly better indication of the spectral distribution curve was obtained by measuring the relative energy in the red, green, and blue regions. The results of these measurements for P-X42 phosphor and the corresponding measurements for P-24 phosphor were as follows:

	P-X42	P-24
Red . . . . .	6 percent	7 percent
Green . . . . .	63 percent	50 percent
Blue . . . . .	31 percent	43 percent

These data suggest that the spectral distribution of P-X42 phosphor has a little more energy in the green band and a little less in the blue band than P-24 phosphor.

P-X42 phosphor did not age or burn during any of the tests. Several attempts were made to damage the screen by scanning at very low speed with high repetition rates. These attempts succeeded in discoloring the screen slightly along the scan line, but failed to cause a measurable change in light output or any other characteristic. The beam was never held stationary at high current, however. Visually, the phosphor never appeared to be overloaded. Therefore, no maximum load factors can be recommended for this phosphor.

#### P-SP Phosphor

Table 6 shows the results of the pulse test on P-SP phosphor. Allowing for some scatter in the data from experimental errors, several conclusions can be drawn. The rise curve becomes steeper at its leading edge as the beam energy decreases. The decay time increases significantly with increasing dwell time and increases very slightly with decreasing beam energy.

TABLE 6. - PULSE DATA FOR P-SP PHOSPHOR

Relative light output	Rise time, $\mu\text{sec}$ , to -			Decay time, $\mu\text{sec}$ , to -		Pulse width, $\mu\text{sec}$
	50 percent	75 percent	100 percent	50 percent	25 percent	
1	0.070	0.26	2.0	0.055	0.15	10
				.055	.15	1
				.04	.09	.1
1/4	0.025	0.20	2.0	0.05	0.15	10
				.05	.15	1
				.04	.09	.1
1/16	0.010	0.10	2.0	0.06	0.18	10
				.06	.16	1
				.04	.09	.1
1/64	0.010	0.015	2.0	0.06	0.20	10
				.055	.16	1
				.04	.09	.1

Figure 14 shows the frequency response obtained from P-SP phosphor. All tests produced gain curves that were virtually identical, which shows that the gain does not depend on dwell time. The bandwidth of P-SP phosphor is 21 megahertz.

The light output of P-SP phosphor did not vary more than 10 percent for any of the scan speeds; thus, it was not necessary to plot a light-output curve.

The gain and slit-scan tests were also conducted on each color of the light from P-SP phosphor. Figure 15 shows the frequency responses obtained. The bandwidth of blue light is 25 megahertz, and the bandwidth of red and green light is 19 megahertz.

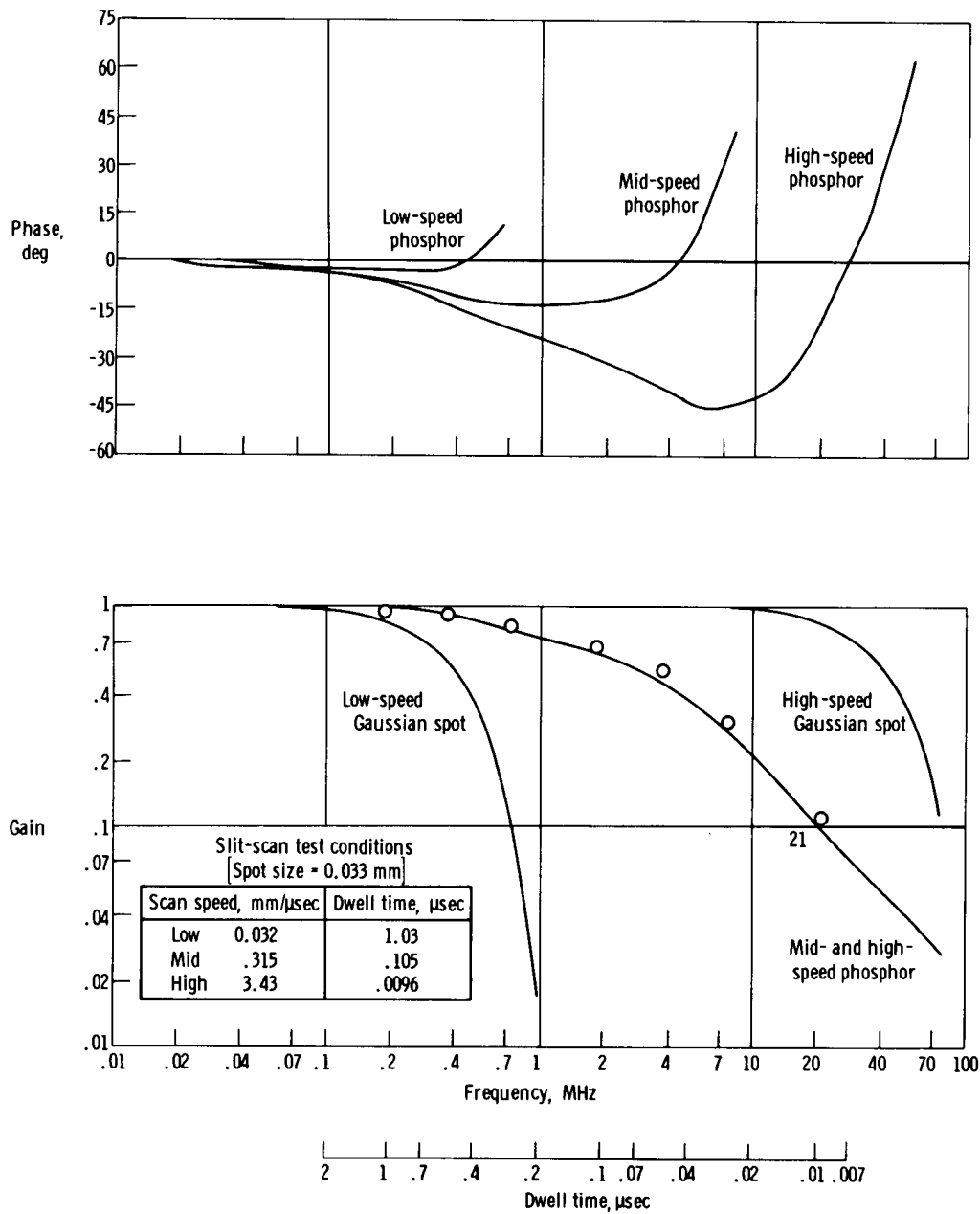


Figure 14. P-SP phosphor frequency response.



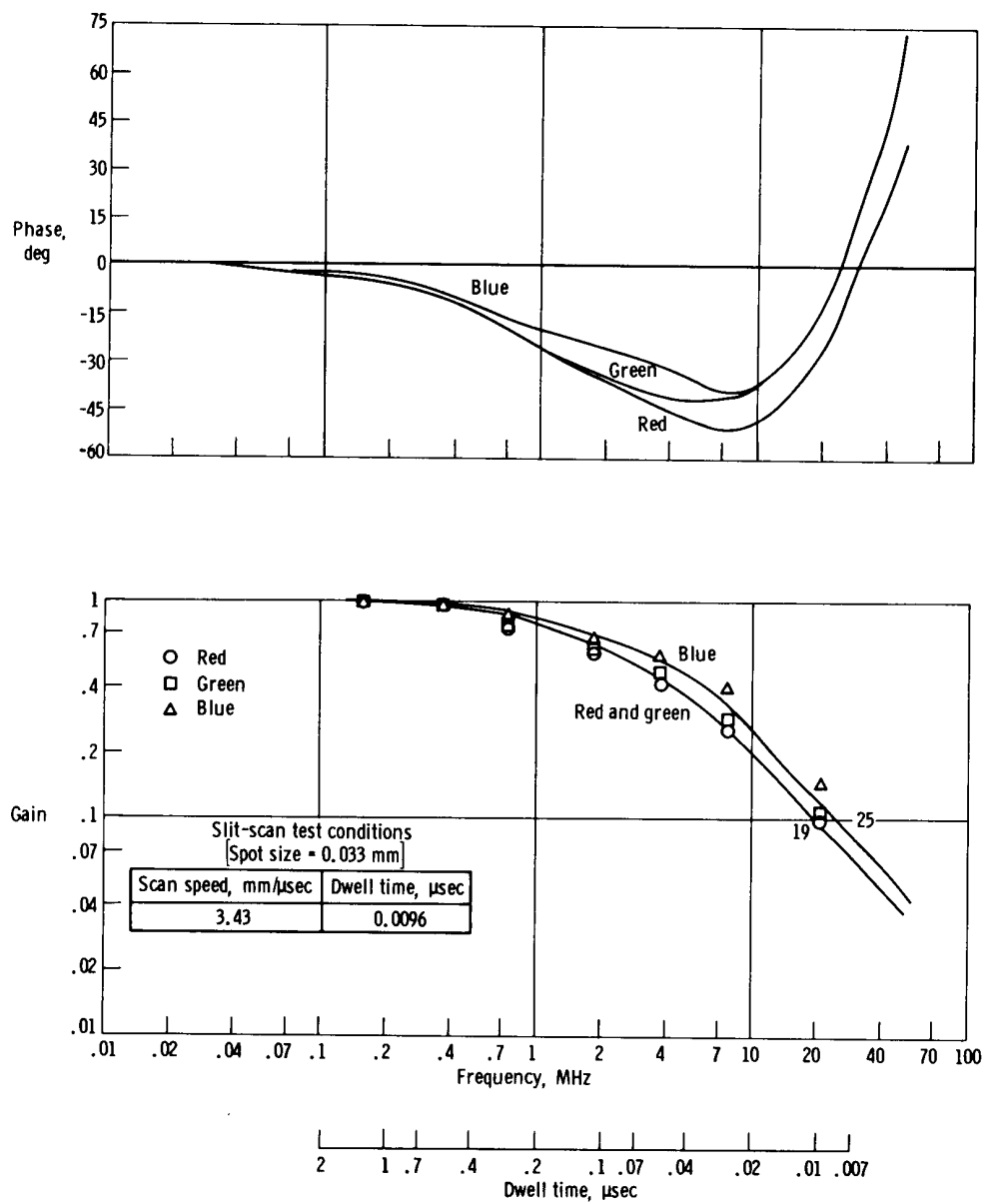


Figure 15. P-SP phosphor color frequency response.

The relative amounts of each color remained constant for all test conditions at the following values:

Red . . . . .	23 percent
Green . . . . .	44 percent
Blue . . . . .	33 percent

The following characteristics were measured:

Spot size in direction of scan . . . . .	0.033 mm
Spot size normal to scan . . . . .	0.066 mm
Noise level . . . . .	20 percent
Color of emitted light . . . . .	Yellowish white

This phosphor did not burn during any of the tests. An aging test was conducted which consisted of scanning at the same conditions as in the low-speed slit-scan test for about 2 hours. The light output reduced about 20 percent. A visual observation suggested that the phosphor was loaded a little too heavily for satisfactory screen life. These factors resulted in a maximum recommended loading of  $0.004 \mu\text{A}/\text{mm}^2$  at a dwell time of 0.5 microsecond.

#### Comparison of the Phosphors

Several general results seem to be applicable to most of the tested phosphors. The repetition rate, for example, did not appear to affect any of the characteristics of these phosphors as long as the average loading did not cause burning. Possibly this result is true only as long as the rest period between excitations is long compared to the decay time. No repetition rates were applied in excess of 1 kilohertz.

The rise and decay times measured by the pulse tests do not seem to be precisely related to the bandwidths found in the other tests. For example, the pulse tests showed that the decay time of P-16 phosphor at maximum loading and minimum pulse width was 0.032 microsecond to 50 percent and 0.060 microsecond to 25 percent of the brightness at the end of the pulse. The corresponding decay times for P-37 phosphor were 0.03 microsecond and 0.07 microsecond. The bandwidths were 22 megahertz for P-16 phosphor and 34 megahertz for P-37 phosphor. Clearly, the relative decay times do not suggest that P-37 phosphor had a bandwidth 50 percent higher than that of P-16 phosphor.

The decay times of all of the phosphors increased with increasing pulse width at all levels of electron beam energy. However, this characteristic never caused an appreciable loss in bandwidth at long dwell times. In fact, two phosphors actually had higher bandwidths at long dwell times. These contradictions are probably the result of not considering the entire nonlinear time and load characteristics of the rise and decay curves.

All phosphors except P-24 seemed to have bandwidths that did not change appreciably with electron beam current density. The decay times at minimum pulse width also showed little or no change as the light output changed from maximum to one-fourth maximum (these conditions most closely approximate the scanning conditions)

for all phosphors except P-24. Both of these results support the conclusion that, with the exception of P-24 phosphor, the bandwidths are either constant or depend primarily on dwell time for the loadings applied in these tests. The bandwidth of P-24 phosphor depends on both beam current density and dwell time. Although it was not actually measured, the data suggest that the bandwidth of P-24 phosphor may depend on the product of dwell time and beam current density, which is essentially total energy per unit area delivered in each sweep.

No attempts were made to study the effects of accelerating voltage on the bandwidth. Although it is assumed that the phosphor is sensitive to total beam energy only, it may make a difference if a fixed amount of energy is received as high voltage and low current one time and high current and low voltage another time.

Table 7 shows some comparative data for the phosphors tested. Two maximum recommended load factors are shown for each phosphor. The first is the one determined from long dwell times. The second is intended to apply to short dwell times and accounts for the gains or losses of light output that resulted from changing the dwell time. Appendix B presents the equation required to adjust the load factor.

TABLE 7. - COMPARISONS OF SIX PHOSPHORS

Phosphor	Bandwidth, MHz	Maximum recommended load factor, $\mu\text{A}/\text{mm}^2$ , at a dwell time of -		Relative noise	Factors that affect the bandwidth	Remarks
		0.5 $\mu\text{sec}$	0.015 $\mu\text{sec}$			
P-16	22	0.0015	0.002	3.7	Constant	Burns easily and ages rapidly
P-24	5.4 to 12, highly variable	0.003	0.005	6.6	Beam current and dwell time	Highly resistant to burning and aging
P-36	12	0.003	0.002	2.7	Dwell time	Strong spectral shift with load variation
P-37	34	0.005	0.002	4.3	Constant	Light output reduces for short dwell time
P-X42	Probably over 100	Indeterminate		36.0	None that were measurable	Too noisy to be usable, inefficient
P-SP	21	0.004	0.004	4.4	Constant	Very wide visible spectrum

The relative noise was computed by multiplying the measured noise level by the approximate spot area and scaling the product arbitrarily. This multiplication is intended to account for the effect of spot size on screen noise. The measured screen noise is assumed to be inversely proportional to spot area. The numerical values of the relative noise have no absolute meaning. They only serve to compare the phosphors.

The relative noise is not necessarily a fixed characteristic of a phosphor. Ignoring P-X42 phosphor, the highest relative noise was measured for P-24 phosphor. However, the second cathode-ray tube that was tested with P-24 phosphor had a much lower relative noise, probably about 1. These two cathode-ray tubes were very different in quality and price, and one of the higher quality features of the second tube was the reduced screen noise. Thus it is possible that the relative noise figures are only indicative of the workmanship applied to the various screens.

The maximum recommended load factors are surprisingly similar. They indicate that, of the phosphors tested, none can safely produce vastly more light than another.

Since light output usually determines the signal-to-noise ratio, and, since the signal-to-noise ratio is usually proportional to the square root of the light output, it is concluded that signal-to-noise ratios are likely to be within a factor of 2 of each other, regardless of the phosphor used.

The bandwidths shown in table 7 were measured by using only one sample of each phosphor except P-24, for which two samples were used. Other studies, such as that described in reference 2, have shown that decay time can vary with such factors as aging and temperature. Also, different samples of the same type of phosphor may display large variations in decay time. These variations suggest that the bandwidths may also vary in a similar manner. Thus the bandwidths measured in this experiment may not necessarily apply to all samples of a particular phosphor type.

P-X42 phosphor displayed a combination of very desirable and very undesirable features. The screen noise appeared to be the worst feature. Most probably, this experimental phosphor did not lend itself to known screen-making methods. It was also less efficient than the other phosphors tested. This disadvantage, though, did not appear to be as serious as the screen noise. The phosphor resisted burning well and would probably have produced a reasonable amount of light if a cathode-ray tube were used that could have produced high beam energy. The very high bandwidth is, of course, an extremely desirable feature that could greatly increase the capability of flying-spot scanners.

#### Bandwidth Maximization

One of the most common problems facing the designer of a flying-spot scanner is maximizing the bandwidth. This can be done by scanning at a speed just high enough to make the spot gain near unity at the highest frequency that the phosphor can produce. Scanning at higher speeds will not improve the scanning bandwidth. In fact, for such phosphors as P-24 and P-36, excessive scan speed can actually reduce the scanning bandwidth because the phosphor bandwidths decrease with decreasing dwell time. Perhaps a good way to select a dwell time is to position the -3-dB point on the gain curve of a Gaussian spot at the frequency where the phosphor gain is 0.1. As shown in appendix C, the -3-dB point of a Gaussian spot is where the product of frequency and dwell time is 0.3. Thus the optimum dwell time for a particular phosphor is 0.3 divided by its bandwidth. The optimum scan speed then becomes the spot size divided by dwell time.

#### SUMMARY OF RESULTS

A series of tests on six phosphors to determine their frequency responses and other properties applicable to flying-spot scanners yielded the following results:

The five production phosphors tested, P-16, P-24, P-36, P-37, and P-SP, had some characteristics in common. They produced similar amounts of light, as seen by a detector with S-20 spectral response. The maximum light produced was only  $3 \frac{1}{3}$  times the minimum. The frequency responses of these phosphors did not change as a function of repetition rate if the rate was below 1 kilohertz and the phosphors were not burned by overloading.

The frequency response of P-16 phosphor did not vary with changes in beam current or dwell time. The bandwidth (the frequency at which the gain is 0.1) was 22 megahertz. The light output increased with constant beam current and decreasing dwell time. Since the phosphor burned easily and aged rapidly, it could not safely produce as much light as the other phosphors at long dwell times.

The frequency response of P-24 phosphor varied with changes in beam current and dwell time. Both increasing beam current and increasing dwell time caused increases in the bandwidth. Bandwidths were measured that ranged from 5.4 megahertz to 12 megahertz. The light output increased with constant beam current and decreasing dwell time. Since the phosphor was highly resistant to aging and burning, it could produce more light than the other phosphors at short dwell times.

The frequency response of P-36 phosphor varied with changes in dwell time but not with changes in beam current. The maximum realizable bandwidth at optimum dwell time was 12 megahertz. The light output had a relative maximum around a dwell time of 0.1 microsecond, decreasing for other dwell times. It exhibited a spectral shift toward the red with decreasing dwell time. This phosphor produced moderate amounts of light and had moderate resistance to burning and aging.

The frequency response of P-37 phosphor did not vary with changes in beam current or dwell time. The bandwidth was about 34 megahertz. The light output had a relative maximum at a dwell time of 0.5 microsecond, decreasing for other dwell times. This phosphor had moderately high resistance to burning and aging and could produce more light than the other phosphors at long dwell times.

The frequency response of P-SP phosphor did not vary with changes in beam current or dwell time. The bandwidth was 21 megahertz. The light had a wider spectral distribution in the visible range than any of the others, and both light output and spectral distribution remained constant at constant beam current and varying dwell time. This phosphor produced a moderately high light output and had moderately high resistance to burning and aging.

P-X42, an experimental phosphor, had a bandwidth so high that its frequency response could not be measured. The bandwidth is known to be at least 80 megahertz and may be well in excess of 100 megahertz. No changes in light output as a function of dwell time were measured. Although this phosphor was highly resistant to burning and aging, it did not produce as much light as the other phosphors tested. Also, the screen was so noisy that this cathode-ray tube would not be usable in a flying-spot scanner.

Flight Research Center,  
National Aeronautics and Space Administration,  
Edwards, Calif., May 20, 1970.

## APPENDIX A

### PHOSPHOR AND PHOTOCATHODE SPECTRAL CURVES

The spectral emission curves of five of the phosphors tested and the spectral sensitivity curve of an S-20 photocathode are shown in figure 16. These curves were furnished by cathode-ray tube and photomultiplier tube manufacturers.

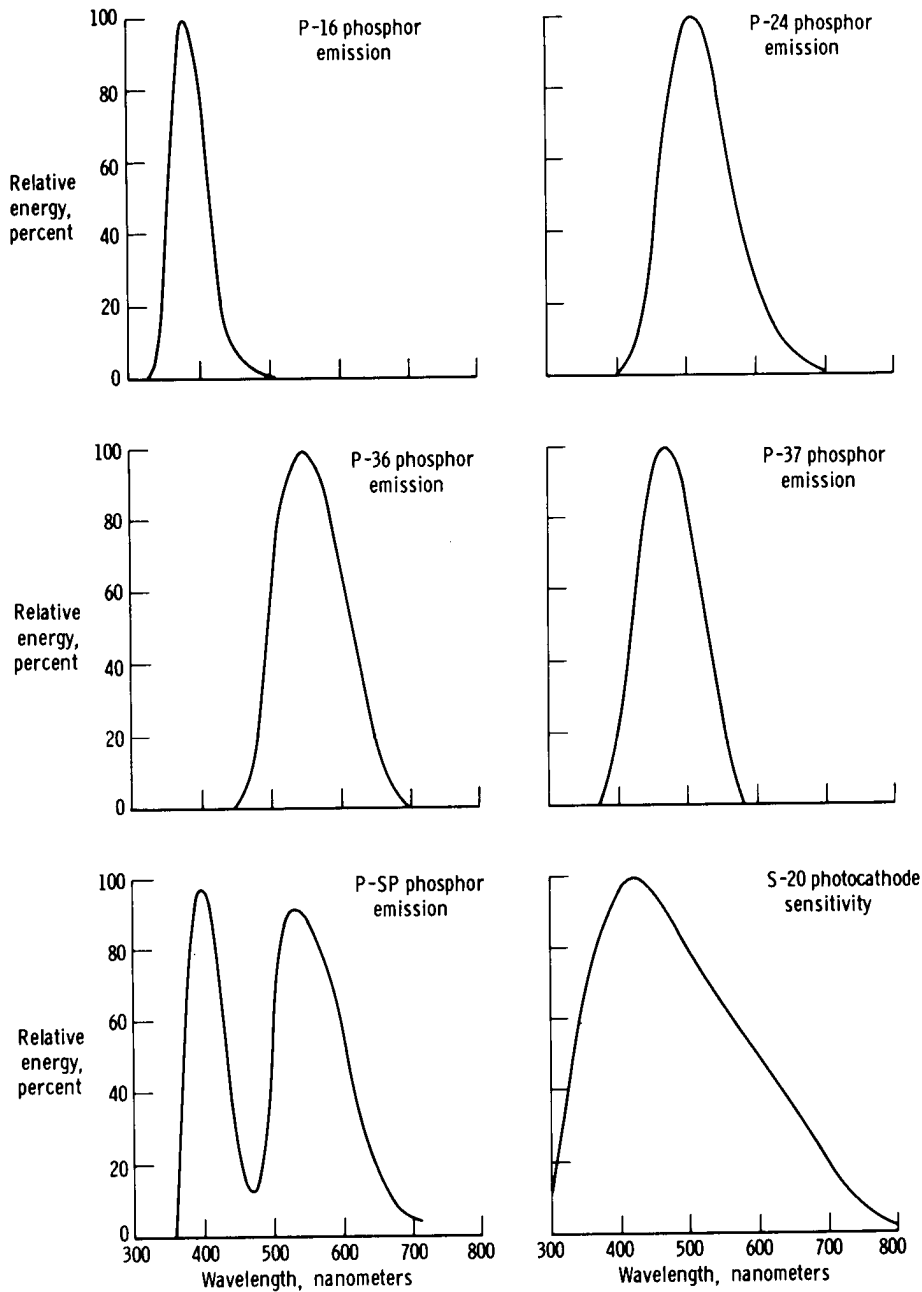


Figure 16. Phosphor and photocathode spectral curves.

## APPENDIX B

### DERIVATION OF PHOSPHOR LOAD FACTOR

A load factor can be computed for a phosphor based on light output. The load factor, which is analogous to the average brightness of a scan line, is the average light output per unit area. Assuming that the duty cycle is the product of dwell time and repetition rate, and assuming that the spot area is approximately its width times its height, the load factor becomes

$$F = \frac{lnT}{wh}$$

where

F = load factor

l = instantaneous light output

n = repetition rate of the scan

T = dwell time of the electron beam,  $w/v$

w = spot size between the half-amplitude points in the direction of scan (width)

v = scan speed

h = spot size between the half-amplitude points normal to the scan (height)

This load factor, which has dimensions of light output per unit area, is useful as a measure of the maximum loading that a phosphor can withstand before it burns.

Some phosphors change their light output when the dwell time is changed, even though the energy loading applied to the screen is not changed. P-24 phosphor, for example, will increase its light output by about 75 percent if the dwell time is reduced from 1 microsecond to 0.02 microsecond, even though the beam energy is constant and the repetition rate is increased to compensate for the decreased dwell time. For such phosphors, the maximum safe load factor varies in proportion to the light output. Therefore, for any dwell time  $t$ , the load factor becomes

$$F = F_1 \frac{l}{l_1}$$

where

$F_1$  = load factor at dwell time  $t_1$

l = relative light output at dwell time  $t$

$l_1$  = relative light output at dwell time  $t_1$

The relative light output as a function of dwell time can be obtained from the light-output curves in the main body of this paper.

## APPENDIX C

### DERIVATION OF THE FREQUENCY RESPONSE OF A GAUSSIAN SPOT

The frequency response of a Gaussian spot is found by taking the Fourier transformation of the spot profile. The Fourier transformation  $H$  (functional notation) is defined as

$$H(f) = \int_{-\infty}^{\infty} e^{-i2\pi ft} G(t) dt$$

where

$$i = \sqrt{-1}$$

$f$  = temporal frequency

$t$  = time

$G$  = amplitude of a Gaussian distribution (functional notation)

A Gaussian distribution is defined as

$$G(x) = \frac{1}{\sqrt{2\pi\sigma^2}} e^{-\frac{x^2}{2\sigma^2}}$$

where

$x$  = distance coordinate

$\sigma$  = one standard deviation on a Gaussian distribution based on distance

The distance between the half-amplitude points is

$$w = 2\sigma\sqrt{2\ln 2}$$

where

$w$  = spot size between half-amplitude points

Replacing  $\sigma$  in the expression for the Gaussian distribution results in

$$G(x) = \sqrt{\frac{4\ln 2}{\pi w^2}} e^{-\frac{4x^2 \ln 2}{w^2}}$$



## APPENDIX C

The spatial parameters are related to the temporal parameters by the expressions

$$\begin{aligned} G(t) &= vG(x) \\ w &= vT \end{aligned} \tag{1}$$

$$\begin{aligned} x &= vt \\ f &= vf_s \end{aligned} \tag{2}$$

where

$v$  = spot velocity (scan speed)

$f_s$  = spatial frequency

$T$  = spot dwell time between half-amplitude points

Thus the Gaussian distribution becomes

$$G(t) = \sqrt{\frac{4\ln 2}{\pi T^2}} e^{-\frac{4t^2 \ln 2}{T^2}}$$

Taking the Fourier transformation results in

$$\begin{aligned} H(f) &= \int_{-\infty}^{\infty} e^{-i2\pi ft} \sqrt{\frac{4\ln 2}{\pi T^2}} e^{-\frac{4t^2 \ln 2}{T^2}} dt \\ H(f) &= e^{-\frac{\pi^2 f^2 T^2}{4\ln 2}} \approx e^{-3.56(fT)^2} \end{aligned} \tag{3}$$

Equations (1) and (2) show that

$$f_s w = \left(\frac{f}{v}\right)(vT) = fT \tag{4}$$

Therefore, the nondimensional product of temporal frequency and dwell time in equation (3) can be replaced by the nondimensional product of spatial frequency and spot size. Figure 17 shows a graph of equation (3). It is seen that the gain of a Gaussian spot is 3 dB down when  $fT$  (or  $f_s w$ ) is approximately 0.3. The phase is zero because equation (3) contains no complex parts.

Equation (1) also shows that

$$f = \frac{(fT)v}{w}$$

## APPENDIX C

This expression can be used to convert the nondimensional abscissa of figure 17 to a frequency abscissa if the spot size and scan speed are known.

Thus it is shown that the bandwidth of a Gaussian spot is directly proportional to scan speed and inversely proportional to spot size.

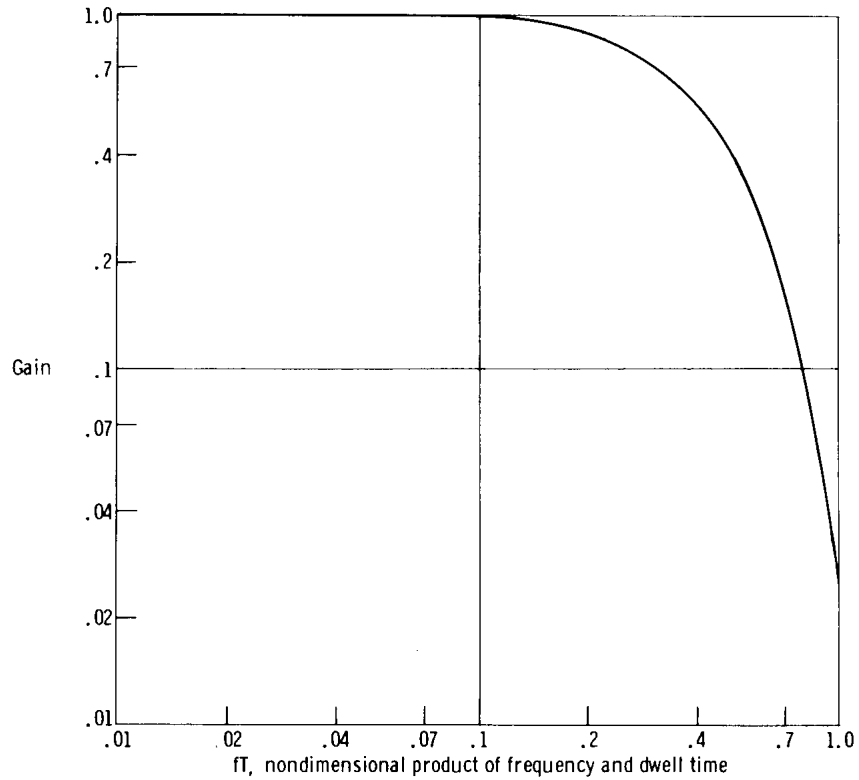


Figure 17. Gain of a Gaussian spot.

## REFERENCES

1. Knudson, D. R.; Teicher, S. N.; Reintjes, J. F.; and Gronemann, U. F.: Experimental evaluation of the resolution capabilities of image-transmission systems. *Information Display*, Sept./Oct. 1968, pp. 31-43.
2. Pfahnl, Arnold: Properties of Fast-Decay Cathode-Ray Tube Phosphors. *Bell System Tech. J.*, vol. XLII, no. 1, Jan. 1963, pp. 181-201.
3. Bryden, J. E.: Some Notes on Measuring Performance of Phosphors Used in CRT Displays. *Technical Session Proceedings, Seventh National Symposium on Information Display*, 1966, pp 83-103.